

## SPECTRAL EVOLUTION OF YOUNG STELLAR OBJECTS

FRED C. ADAMS, CHARLES J. LADA, AND FRANK H. SHU

Institute for Theoretical Physics, Santa Barbara

Received 1986 March 27; accepted 1986 July 1

### ABSTRACT

We suggest an evolutionary sequence, from protostars to pre-main-sequence stars, for the classification of young stellar objects. This sequence is derived by comparing the predictions of the theoretical models of Adams and Shu with the morphological classification scheme of Lada and Wilking. We first define the spectral index in the near-infrared and mid-infrared,  $n \equiv d \log (\nu F_\nu) / d \log \nu$ , and then interpret the class of sources with negative spectral indices as protostars. The inferred mass infall rates for these objects are generally consistent with the measured gas temperatures of  $\sim 35$  K in Ophiuchus and of  $\sim 10$  K in Taurus. Fitting the data requires us to adopt cloud rotation rates in Ophiuchus which are typically an order of magnitude greater than in Taurus, and we speculate on the mechanistic origin for this difference. Next, we consider a subclass of T Tauri stars with near-infrared and mid-infrared excesses and positive or zero spectral indices. We find that the objects with the steeper indices can be understood as the postinfall products from the collapse of rotating cloud cores, where the infrared excesses arise from the simple reprocessing of visible stellar photons in optically thick but spatially thin disks. The sources with flatter spectra may require massive accretion disks. Given the existence of protostars and naked star/disk systems, there is a natural interpretation of another subclass of T Tauri stars, those with two peaks in their emergent spectral energy distributions. These are readily explained as intermediate cases in which dust envelopes, optically thin in the infrared, still surround the stars and disks, perhaps because of residual infall. Finally, we find that the theory can be extended to explain the spectral energy distribution of FU Orionis, a famous outburst source. Our model suggests that FU Orionis has a disk, but it offers no discrimination between the competing ideas that the outburst took place on the star or in the disk.

*Subject headings:* infrared: sources — stars: formation — stars: pre-main-sequence

### I. INTRODUCTION

In a survey of the large dense core of the Ophiuchus molecular cloud, Lada and Wilking (1984, hereafter LW) were able to divide its infrared sources into three distinct morphological classes based on the shapes of the observed energy distributions: (a) unidentified objects with negative spectral indices,

$$n \equiv \frac{d \log (\nu F_\nu)}{d \log \nu}, \quad (1)$$

in the mid-infrared and near-infrared (from  $\nu = 10^{13.5}$  to  $10^{14.5}$  Hz, i.e., from  $\lambda = 10$  to  $1 \mu\text{m}$ ); (b) embedded T Tauri stars with mid-infrared and near-infrared excesses that have positive or zero spectral indices; and (c) embedded main-sequence and pre-main-sequence stars, which could be adequately modeled as reddened blackbodies. Thus, class (c) objects are simply young stars with little hot circumstellar dust, with the extinction caused by distant (and hence cool) grains. LW (see also Lada 1986) assumed that the members of class (a), the negatively steep spectrum sources, correspond to protostars, i.e., stars in the process of being made by continuing infall of ambient molecular cloud material, but LW offered no physical explanation for the characteristic shapes of the emergent spectral energy distributions of either the class (a) or class (b) objects. In the interim, the identification of steep-spectrum infrared sources (with  $n < 0$ ) as protostars has been made more secure by the observational finding of Myers *et al.* (1986) that such objects in the Taurus molecular cloud are invariably located near the centers of small ammonia cores. Theoretical modeling by Adams and Shu (1986, hereafter AS) has shown that the prototypical source with a negatively steep spectrum

in Taurus, Haro 6–10, can be readily explained as a rotating and collapsing protostar.

In this paper, we advance the proposal that the LW classes represent an evolutionary progression in the birth of a (low-mass) star. First, the collapse of a cloud core begins, producing (a) a protostar during its main infall phase, i.e., a star and disk embedded in an infalling dust envelope. An intense wind phase then terminates the infall to reveal (b) a newly born star surrounded by a nebular disk. After the disappearance of the disk, the result is (c) an isolated pre-main-sequence or near-main-sequence star (possibly with planetary or stellar companions) contracting in the H-R diagram along a convective-radiative track (Hayashi, Hoshi, and Sugimoto 1962). We seek to demonstrate the validity of this proposal by showing that the emergent spectral energy distributions for each step of the sequence can be explained by a self-consistent theoretical formulation. In § II, we show that the protostar models of AS adequately explain the emergent spectral energy distributions of class (a) sources in both Taurus and Ophiuchus. If the infalling dust envelope is then completely removed (§ III), the spectra of the underlying stars and nebular disks used by AS (see their Appendix) provide a natural explanation for the near-infrared and mid-infrared excesses and the positive spectral indices of class (b) sources. In § IV, we find that the addition of a simple physical model for residual dust envelopes can reproduce the far-infrared excesses (which are manifested in double-peaked energy distributions) found in some of the class (b) sources.

Although the qualitative scheme introduced above could, in principle, be applied equally well to young stellar objects (YSOs) of high mass, we restrict the practical modeling to

systems of low mass. The restriction is made primarily because the protostellar calculations carried out to date have been done most reliably and self-consistently for systems of low mass (e.g., Larson 1969; Winkler and Newman 1980*a, b*; Stahler, Shu, and Taam 1980). The evolution of high-mass stars is more problematic to follow because they inflict severe damage on their surroundings once they begin to acquire large luminosities (e.g., Larson and Starrfield 1971; Kahn 1974; Appenzeller and Tscharnuter 1974; Yorke and Krugel 1977). In addition to the ubiquitous winds which seem to occupy some phase of the life of every YSO, high-mass systems suffer the mechanical back reactions of ionization of the gas (which may recouple the fluid to the ambient magnetic fields) and radiation pressure acting on the inflowing grains. The last effect, in particular, has been ignored in the inflow density profile adopted for our calculations—the semianalytical description given by Terebey, Shu, and Cassen (1984, hereafter TSC) of the gravitational collapse of the slowly rotating core of a molecular cloud. The neglect of the effects of radiation pressure can be shown to be valid for stars less massive than about  $7 M_{\odot}$  under the worst of all circumstances (spherical accretion), as can be seen by the following simple argument.

The rate of momentum transfer per unit mass (averaged over a sphere) to a mixture of gas and dust (assumed to be well coupled dynamically) by a radiation field of spectral energy distribution  $L_{\nu}$  at a distance  $r$  from a protostar is given by

$$\int_0^{\infty} \frac{\kappa_{\nu} L_{\nu}}{4\pi cr^2} dv \approx \frac{\kappa_p(T)L}{4\pi cr^2}, \quad (2)$$

where  $L$  is the bolometric luminosity,  $\kappa_p(T)$  is the Planck mean of the dust opacity (see Fig. 2 of AS), and the protostellar radiation field is assumed to be thermalized to the local dust temperature  $T$ . The last assumption is well justified in the inner portions of the infalling dust envelope which are optically thick where most of the radiative deceleration takes place. In these regions, to a rough order of approximation,  $\kappa_p(T) \approx \kappa_p(T_d)(T/T_d)$  and  $T \approx T_d(r_d/r)^{1/2}$ , where  $T_d$  is the dust destruction temperature ( $\sim 2000$  K) reached at a radius  $r_d$ . Integrated from a large distance to the dust destruction radius, the specific work done by the outwardly directed component of the radiative force equals

$$\int_{r_d}^{\infty} \frac{\kappa_p(T)L}{4\pi cr^2} dr \approx \frac{\kappa_p(T_d)L}{6\pi cr_d}. \quad (3)$$

The use of the Planck mean opacity underestimates the contribution of the direct stellar radiation field seen by the grains just before they cross the dust destruction front; however, the impulse from this effect is small because of the short time required to traverse the finite thickness of the thermalization layer of the photons coming from the central source. Thus, the work done by the radiation field is much less than the gravitational potential  $GM/r_d$  at  $r_d$  if

$$L/M \ll 6\pi cG/\kappa_p(T_d) \approx 700 L_{\odot}/M_{\odot}, \quad (4)$$

where we have assumed  $\kappa_p(T_d) = 30 \text{ cm}^2 \text{ g}^{-1}$  for a cloud of gas and dust with cosmic abundances (see Fig. 2 of AS). Equation (4) holds to a good approximation for Population I stars less massive than about  $7 M_{\odot}$ . The mass limit may be pushed upward if  $\kappa_p(T_d)$  is lower because of metallicity deficiencies (Wolfire and Cassinelli 1986), if rapidly accreting protostars are induced to have luminosities less than their corresponding main-sequence values (S. Stahler 1986, private

communication), or if rotating infall occurs onto a disk of characteristic dimension  $R_c \gg r_d$  and buildup of the central star beyond the spherical limit (4) takes place via disk accretion.

There are other good reasons to restrict our attention initially to low-mass protostars. First, the luminosities of such objects are largely due to accretion, which for fixed mass infall rates  $\dot{M}$ , are monotonically increasing functions of time in the simplest models (see also the discussion of Beichman *et al.* 1986). In particular, the collapse of a singular isothermal sphere has  $\dot{M} = m_0 a^3/G$ , where  $m_0 = 0.975$  and  $a$  is the isothermal sound speed (Shu 1977). A detailed test is possible because systematic differences should exist between the sources in Taurus, where  $a = 0.2 \text{ km s}^{-1}$  on average, and in Ophiuchus, where  $a = 0.35 \text{ km s}^{-1}$  on average. For fixed  $\dot{M}$ , the luminosity of a class (a) source should be an indicator of the evolutionary age of the protostar. Second, it is only for objects less massive than about  $2 M_{\odot}$  (i.e., objects destined to become T Tauri stars) that we have a firm idea of what powers the outflow that eventually reverses the infall and reveals the central object as a visible source. Only in protostars less massive than about  $2 M_{\odot}$  will the onset of deuterium burning drive the interior convection that couples to the field of differential rotation and gives the dynamo action and, presumably, the vigorous surface activity which characterizes the outflow from YSOs of low mass (Shu 1985). Indeed, Shu argued that the identification of the stage of deuterium burning with the removal of the placental material would provide a natural explanation for the insensitivity of the location of the “birthline” for T Tauri stars to the details of the prior accretion phase (e.g., direct infall versus disk accretion; cf. Stahler 1983, 1984; Mercer-Smith, Cameron, and Epstein 1984). This conjecture has now been verified by S. Stahler (1986, private communication) in a series of detailed calculations. Powerful stellar winds may also account for how YSOs of high mass eventually become revealed; however, in such cases, our conception of the detailed mechanism by which such outflows are powered is much more vague (see, e.g., Shu, Lizano, and Adams 1986).

An enigmatic and possibly important phase associated with some YSOs is the FU Orionis phenomenon, the prototype of which is commonly believed to be a T Tauri star that brightened suddenly in 1936–1937 by 5–6 mag. Thus, it is interesting that as a side development of the investigations of this paper, we found (§ V) that a scaled-up version of a simple star-plus-disk model suffices to explain the emergent spectral energy distribution of the FU Orionis system. Unfortunately, the spectrum can be fit theoretically under two extreme assumptions: (1) the disk is passive and merely reprocesses the visible radiation of its central star, and (2) the disk is active and provides all the luminosity of the system via a conventional accretion scenario. Thus, although these models offer strong support that there must be a disk around this peculiar object, they do not discriminate between the competing views which suggest that the outburst took place on the star (for a review, see Herbig 1977) or in the disk (e.g., Lin and Papaloizou 1985; Hartmann and Kenyon 1985).

## II. PROTOSTARS

In this section, we compare observed spectra of class (a) sources with the models of rotating protostars developed by TSC and AS. The theoretical models are characterized by five parameters, the instantaneous mass  $M$  of the protostellar

system, the isothermal sound speed  $a$ , the angular velocity  $\Omega$  of the parent molecular cloud core, and the efficiencies  $\eta_*$  and  $\eta_D$  with which the star and disk dissipate the energy of differential rotation. In addition, the measured energy distribution depends on the angle  $\theta$  between the observational line of sight and the rotational axis of the system.

The viewing direction  $\theta$  is not generally known for most protostellar candidates; fortunately, the emergent spectral energy distribution is not very sensitive to the choice of  $\theta$ , provided the disk is not seen edge-on. Thus, unless specifically stated otherwise, we make our comparisons for the choice  $\theta = 45^\circ$ . The isothermal sound speed  $a$  of the surrounding molecular cloud is calculable from the gas temperatures:  $\sim 10$  K in Taurus as measured in CO and NH<sub>3</sub> (Myers and Benson 1983), and  $\sim 35$  K in Ophiuchus as measured in CO (Lada and Wilking 1980; Loren, Sandqvist, and Wootten 1983). The CO measurements refer to less dense regions, and their line widths exhibit a nonnegligible "turbulent" contribution. The NH<sub>3</sub> measurements refer to the cloud cores, and in Taurus their line widths are nearly thermal. We assume the same will turn out to be true in Ophiuchus and adopt effective sound speeds of  $a = 0.2 \text{ km s}^{-1}$  in Taurus and  $a = 0.35 \text{ km s}^{-1}$  in Ophiuchus.

Given  $a$ , the three quantities  $M$ ,  $\eta_*$ , and  $\eta_D$  combine to produce essentially a single observable, the total accretion luminosity  $L = L_* + L_D$ , where the intrinsic stellar and disk luminosities,  $L_*$  and  $L_D$ , are given by equations (33a) and (33b) of AS. In the limit where the stellar radius  $R_*$  is much less than  $R_C$ , as is nearly true for all our models,  $L_*$  and  $L_D$  have the approximate expressions:

$$L_* \approx \frac{1}{2} \eta_* \eta_D^2 L_0, \quad (6a)$$

$$L_D \approx \frac{1}{2} \eta_D L_0, \quad (6b)$$

where the spherical accretion luminosity  $L_0$  has been taken in this work to equal (see eqs. [28] and [23] of AS):

$$L_0 = G\dot{M}/R_* = 72 L_\odot (a/0.35 \text{ km s}^{-1})^2 (M/M_\odot). \quad (7)$$

From a pure modeling viewpoint, therefore,  $\eta_*$  and  $\eta_D$  may be regarded as merely parameters which characterize the actual  $L$  as a fraction of its spherical infall value and the relative contributions to  $L$  from the star and disk. The theory is incomplete in that we have no mechanistic means at present to specify a priori the values of  $\eta_*$  and  $\eta_D$ ; for sake of definiteness in the empirical modeling, we set  $\eta_* = \frac{1}{2}$ ,  $\eta_D = 1$ .<sup>1</sup> Then, for fixed  $a$ , we vary  $M$  to match the observed bolometric luminosity  $L$ . This leaves a single free parameter, the angular velocity  $\Omega$ , with which to fit the observed spectral *shape*—i.e., the slope and breadth of the energy distribution and the depth of the 10  $\mu\text{m}$  silicate absorption feature. Observations of the angular velocity  $\Omega$  in the surrounding cloud envelope would provide a partial check on the validity of this approach.

<sup>1</sup> The flow of the disk mass entirely onto the star would make the underlying dynamics of the adopted infall model fully self-consistent (inner gravitational potential taken to be that of a point mass); however, we shall present indirect evidence in § VI that some disks around T Tauri stars may have masses comparable to the stars, implying that  $\eta_D$  may be of order  $\frac{1}{2}$  when averaged over the infall phase. During the outflow phase, deuterium burning contributes interior luminosity which will affect the effective value of  $\eta_*$ . If  $(\eta_*, \eta_D)$  equals (1.0, 0.5) rather than (0.5, 1.0), the derived values of  $M$  would need to be adjusted upward by a factor 2.0 (to recover the same  $L$ ), and  $\Omega$ , downward by a factor of 4.0 (to recover the same column density in eq. [14]), if nearly the same fits as shown in the figures are desired.

In AS, the emergent spectral energy was computed at the radius

$$r_2 \equiv 0.4GM/a^2,$$

which corresponds to the rough boundary between the freely falling inner region and the ambient cloud (see Shu 1977). In Ophiuchus, where  $a$  is substantially larger than in Taurus, this choice is inappropriate for two reasons: (1) the radius  $r_2$  is substantially smaller than the beam size of IRAS at 100  $\mu\text{m}$ , and (2) there can be additional material beyond a distance  $r_2$  from the infrared source. In this paper, we take both effects into account by calculating the emergent spectral energy distribution at a radius  $r_3 = 2 \times 10^{17}$  cm from the protostar. This change is minor for Taurus (except at the longest wavelengths), but it is an important consideration for Ophiuchus.

Because  $r_3$  is significantly greater than the radius  $r_2$  inside which the infall solution can be approximately treated as free-fall, we need to extend the functional form of the density profile used by AS. This extension is carried out by adopting the self-similar global solutions of Shu (1977) and TSC for the gravitational collapse of a (slowly rotating) singular isothermal sphere. We can effect a smooth transition between the different flow regimes at time  $t = M/\dot{M} = GM/m_0 a^3 < \Omega^{-1}$  by adopt-

$$\rho(r, \theta) = Cr^{-3/2} \mathcal{R}(u, \theta) \mathcal{B}(x), \quad (8)$$

where  $C \equiv m_0 a^3 / 4\pi(2GM)^{1/2}$ . The dimensionless function  $\mathcal{R}(u, \theta)$  contains the effects of rotation;  $u \equiv r/R_C$  is a dimensionless radial coordinate; and  $R_C$  is the centrifugal radius

$$R_C \equiv G^3 M^3 \Omega^2 / 16a^8. \quad (9)$$

The functional form of  $\mathcal{R}(u, \theta)$  can be obtained from equations (84), (85), (88), and (92) of TSC as

$$\mathcal{R}(u, \theta) = \left( \frac{2\mu_0}{\mu_0 + \mu} \right)^{1/2} \left[ 1 + \frac{2}{u} P_2(\mu_0) \right]^{-1}, \quad (10a)$$

where  $P_2(\mu_0) = (3\mu_0^2 - 1)/2$  is the Legendre polynomial of order 2 and  $\mu_0$  is the cosine of the angle  $\theta_0$  that a parabolic fluid trajectory, currently passing through the position  $u$  and  $\mu \equiv \cos \theta$ , initially made with respect to the rotation axis. As a function of  $u$  and  $\mu$ , the quantity  $\mu_0$  satisfies the cubic equation,

$$\frac{\mu_0(1 - \mu_0^2)}{\mu_0 - \mu} = u. \quad (10b)$$

The root of this cubic which has physical significance possesses the properties:  $\mu_0 \rightarrow \mu$  for  $u \rightarrow \infty$  (all parabolic streamlines are straight and radial at infinity);  $\mu_0 \rightarrow \mu^{1/3}$  for  $u \rightarrow 1$  (notice the strong convergence of streamlines at the centrifugal barrier where half of the initial streamlines,  $|\mu_0| \leq \frac{1}{2}$ , are mapped to an equatorial belt covering only one-eighth of the sky,  $|\mu| \leq \frac{1}{8}$ ); and  $\mu_0 \rightarrow 1$  for  $u \rightarrow 0$  (only nearly polar streamlines can approach the origin and fall directly on the star if  $R_* \ll R_C$ ). Along the polar axis  $\mu = 1$ ,  $\mu_0 = 1$ ; thus,  $\mathcal{R} = u/(2 + u)$ . In the equatorial plane  $\mu = 0$ ,  $\mu_0 = (1 - u)^{1/2}$  for  $u \leq 1$  and  $\mu_0 = 0$  for  $u \geq 1$ ; thus,  $\mathcal{R} = 2^{-1/2}u/(1 - u)$  for  $u < 1$  and  $\mathcal{R} = u/(u - 1)$  for  $u > 1$ . As Cassen and Moosman (1981) have already noted, the pileup of streamlines at the centrifugal barrier formally leads to an equatorial ring of infinite density (but zero mass) at  $u = 1$ ; the singularity would be removed by a disk of finite thickness whose outer edge had spread beyond  $R_C$  because of viscous effects or other mechanisms of internal angular-momentum transport.

The function  $\mathcal{B}(x)$  in equation (8) incorporates the dynamics of the expansion wave which initiates the infall; it is given by

$$\mathcal{B}(x) \equiv (2x^3/m_0)^{1/2}\alpha(x), \quad (11)$$

where  $x \equiv r/r_s$  measures the radial distance in units of the radius of the expansion wavefront,  $r_s = at = GM/m_0 a^2$ , and  $\alpha(x)$  is the function tabulated in Table 1 of Shu (1977) for  $x \leq 1$ . For  $x \ll 1$ ,  $\alpha(x) \approx (m_0/2x^3)^{1/2}$ ; for  $x \lesssim 1$ ,  $\alpha(x) \approx 2/x$ ; and for  $x \geq 1$ ,  $\alpha(x) = 2/x^2$ . Thus, in the limit of small  $x$  (i.e.,  $r \ll r_2$ ),  $\mathcal{B}(x) \rightarrow 1$  so that equation (8) reduces to the rotating free-fall expression used by AS. In the limit of large  $x$  (i.e.,  $r \gg r_2$ ), the density becomes that of the singular isothermal sphere from which the collapse began:  $\rho \rightarrow a^2/2\pi Gr^2$  (for  $r < a/\Omega$ ).

Following the prescription given by AS, we compute the thermal reemission by the dust envelope on the basis of the spherical average of the density distribution (8):

$$\bar{\rho}(r) = Cr^{-3/2}\mathcal{A}(u)\mathcal{B}(x), \quad (12)$$

where  $\mathcal{A}(u)$  is the dimensionless integral

$$\mathcal{A}(u) \equiv \int_0^{\pi/2} \mathcal{B}(u, \theta) \sin \theta d\theta = \int_v^1 \left[ 1 - \frac{1}{2u} (1 - \mu_0^2) \right]^{-1/2} d\mu_0, \quad (13)$$

with the lower limit  $v = 0$  for  $u \geq 1$  and  $v = (1 - u)^{1/2}$  for  $u \leq 1$ . The difference in lower limits arises physically because streamlines from any initial direction can reach  $r \geq R_C$ , but only streamlines coming preferentially from the poles can reach inside the centrifugal radius; this effect depletes the average density inside  $R_C$ , as can be seen explicitly when the last integral in equation (13) is performed analytically, yielding equation (10b) of AS. Since  $\mathcal{A}(u) \approx (2 - 2^{1/2})u$  for  $u \ll 1$  ( $r \ll R_C$ ) and  $\mathcal{A}(u) \approx 1$  for  $u \gg 1$  ( $r \gg R_C$ ), we easily verify, for  $r_d \ll R_C \ll r_2$ , that the average column density of gas and dust (i.e., the average visual extinction) to the central source seen by outside observers obtains most of its contribution near  $r = R_C$ :

$$\int_{r_d}^{\infty} \bar{\rho}(r) dr \approx 3.5CR_C^{-1/2}. \quad (14)$$

The column density along a line of sight which passes through the pole has a value  $\approx 2.2CR_C^{-1/2}$ , a factor of 1.6 less than equation (14). A line of sight which passes exactly through the equatorial plane intercepts a column density which is formally divergent (but only logarithmically), even without considering the additional extinction caused by a protostellar disk.

With the modifications described below, we can use the radiative transfer technique of AS to compute models for a number

of well-observed protostellar candidates. The resultant protostellar parameters are summarized in Table 1. Fitting the observed spectra provides a determination of the total luminosity of these objects that is relatively insensitive to the assumed  $\theta$ , unless  $\theta$  is close to  $90^\circ$ . Even with the removal of the logarithmic divergence of the column density by the insertion of a disk of finite thickness, the visual extinction to the central source can be expected to be much larger than average (by factors of 3 or more), and this holds before the contribution from the disk is considered. The strong gradient of density near  $\theta = 90^\circ$  undoubtedly limits the utility of a spherical averaging technique. However, since the total amount of material at any time in the equatorial "ring" is small, the *thermal emission* from the dust (which is heated by radiation from the entire envelope and is the only part of the calculation where the spherical average is used) should be relatively unaffected when viewed in directions well off the equatorial plane. We might then expect the "equivalent spherical problem" to yield a reasonable approximation to a full radiative transfer calculation in two spatial dimensions and two propagation directions.

With these caveats, we begin by describing a series of three IRAS sources in Taurus—04365+2535, 04016+2610, and 04264+2426 (Haro 6–10)—which were chosen for modeling because narrow-band measurements of the  $10 \mu\text{m}$  silicate absorption feature (an important diagnostic of the conditions in the infalling envelope) existed for them. It is interesting that these three sources can be modeled approximately with the same  $a$  and  $\Omega$  but different  $M$ , indicating that gross properties of the Taurus cloud control the core temperatures (heating and cooling; Lizano and Shu 1986) and rotation rates (magnetic coupling to the envelopes before core collapse; Mouschovias and Paleologou 1979). This allows us to view the models for these three objects as an evolutionary progression, in accordance with the hypothesis that protostars grow by continuous infall from a surrounding envelope of gas and dust (increasing  $M = \dot{M}t$  for fixed  $\dot{M}$ ). The uniformity of  $a$  and  $\Omega$  cannot strictly hold for all the sources in Taurus, for identical molecular cloud cores would presumably produce identical outcomes, and the finished stars in Taurus would then have all the same mass, contrary to observations. Nevertheless, it is intriguing to note the similarity in shape of the spectral energy distributions of the protostellar candidates compiled by Myers *et al.* (1986).

#### a) 04365+2535

The protostellar candidate 04365+2535 in Taurus shows no sign of an outflow (P. Myers 1986, private communication). If we judge its age from its luminosity, it is also the youngest of the three sources we consider in our "evolutionary progres-

TABLE 1  
PARAMETERS FOR PROTOSTAR MODELS

Source	$M$ ( $M_\odot$ )	$a$ (km s $^{-1}$ )	$\Omega$ ( $10^{-14}$ rads s $^{-1}$ )	$L$ ( $L_\odot$ )	$R_C$ (AU)	$3.5CR_C^{-1/2}$ (g cm $^{-2}$ )
04365+2535 .....	0.20	0.20	5.0	3.5	7.4	0.43
04016+2610 .....	0.40	0.20	2.0	7.0	9.5	0.27
Haro 6–10 .....	0.50	0.20	2.0	8.7	18	0.17
WL 16 .....	0.50	0.35	50	27	130	0.34
WL 22 .....	0.60	0.35	10	30	9.0	1.2
Elias 29 .....	1.0	0.35	20	53	170	0.22
IRS 5 L1551 .....	0.675	0.325	10	31	23	0.56
IRS 5 L1551 <sup>a</sup> .....	1.0	0.35	10	28	42	0.42

<sup>a</sup> Dissipation efficiency factors ( $\eta_*$ ,  $\eta_D$ ) taken to be (1.0, 0.5) instead of (0.5, 1.0).

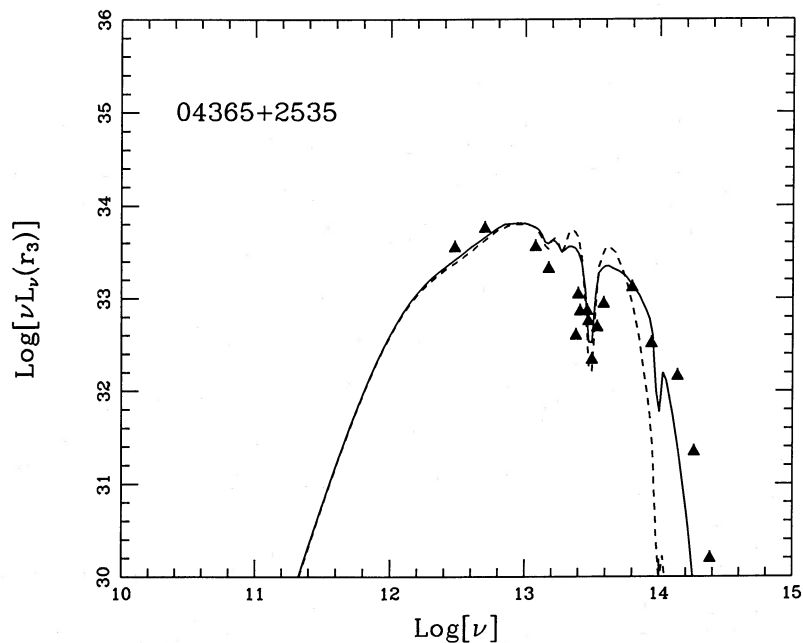


FIG. 1a

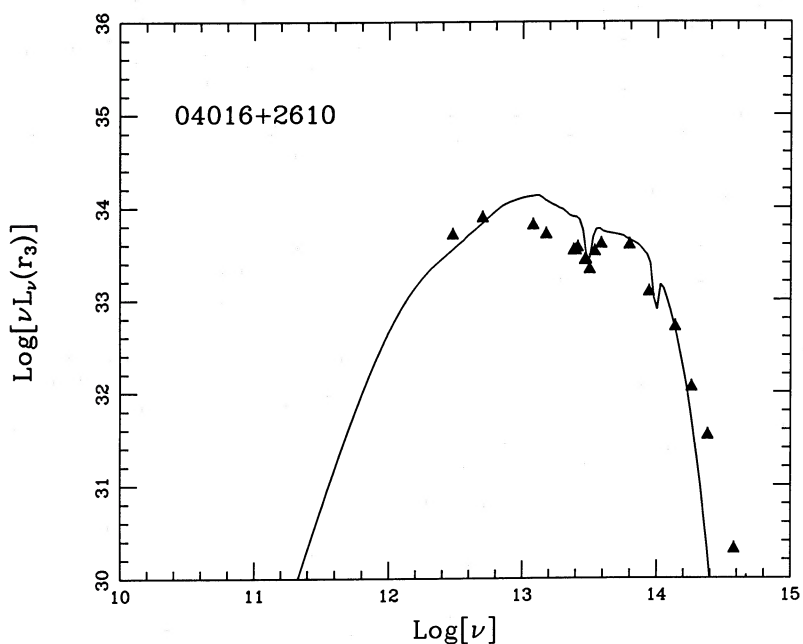


FIG. 1b

FIG. 1.—Comparisons of theoretical emergent spectral energy distributions with observed infrared sources. For all of the sources considered in this paper, we plot  $\log(\nu L_\nu)$  vs.  $\log(\nu)$  with all quantities given in cgs units. The distances to the Taurus and Ophiuchus molecular clouds have been taken to be 160 pc. (a) 04365+2535 (Taurus): data taken from Myers *et al.* (1986); theoretical curves assume  $a = 0.20 \text{ km s}^{-1}$ ,  $M = 0.2 M_\odot$ , and  $\Omega = 2 \times 10^{-14} \text{ rad s}^{-1}$  (dashed curve) or  $\Omega = 5 \times 10^{-14} \text{ rad s}^{-1}$  (solid curve). (b) 04016+2610 (Taurus): data taken from Myers *et al.* (1986); theoretical curve assumes  $a = 0.20 \text{ km s}^{-1}$ ,  $M = 0.4 M_\odot$ , and  $\Omega = 2 \times 10^{-14} \text{ rad s}^{-1}$ .

sion." Adopting  $a = 0.20 \text{ km s}^{-1}$ , we easily calculate from equations (6) and (7) that a value of about  $M = 0.2 M_\odot$  is needed to reproduce the observed luminosity. If  $\Omega$  is then chosen to have the value,  $2 \times 10^{-14} \text{ rad s}^{-1}$ , appropriate for Haro 6–10, we obtain the dashed curve in Figure 1a. This curve has a silicate absorption feature at  $10 \mu\text{m}$  which is a little too deep and an overall spectral shape which is a little too narrow. A better fit to both can be obtained by increasing  $\Omega$  to  $5 \times 10^{-14} \text{ rad s}^{-1}$ , which gives the solid curve in Figure 1a.

The quality of the fits in Figure 1a and elsewhere in this paper has been judged purely by eye. Moreover, our search of parameter space has been restricted primarily to the use of relatively "round" numbers. Given the uncertainties attached to the parameters  $\eta_*$  and  $\eta_D$ , a finer analysis is not justified at this stage of the development of the theory. Some feeling for the degree of nonuniqueness associated with our procedure for estimating  $M$ ,  $a$ , and  $\Omega$  can be obtained from our later discussion of IRS 5 L1551.

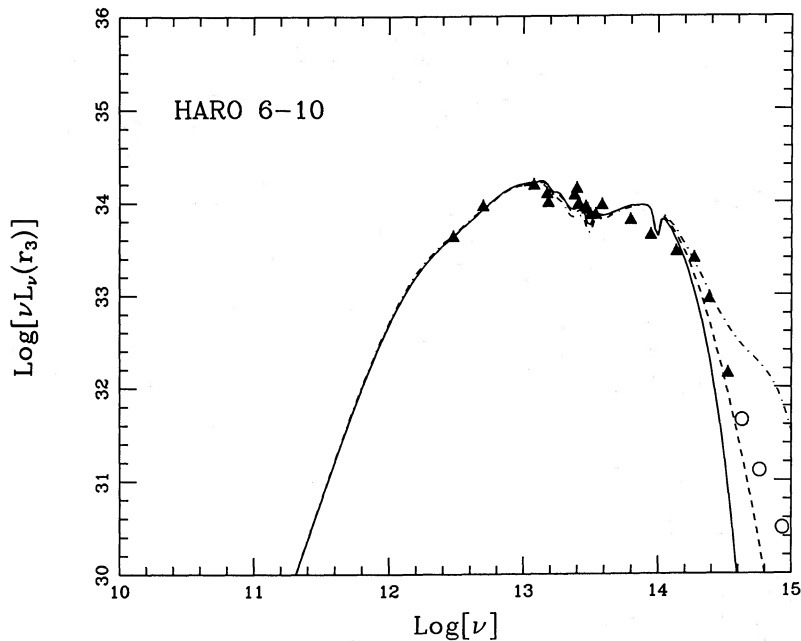


FIG. 1c

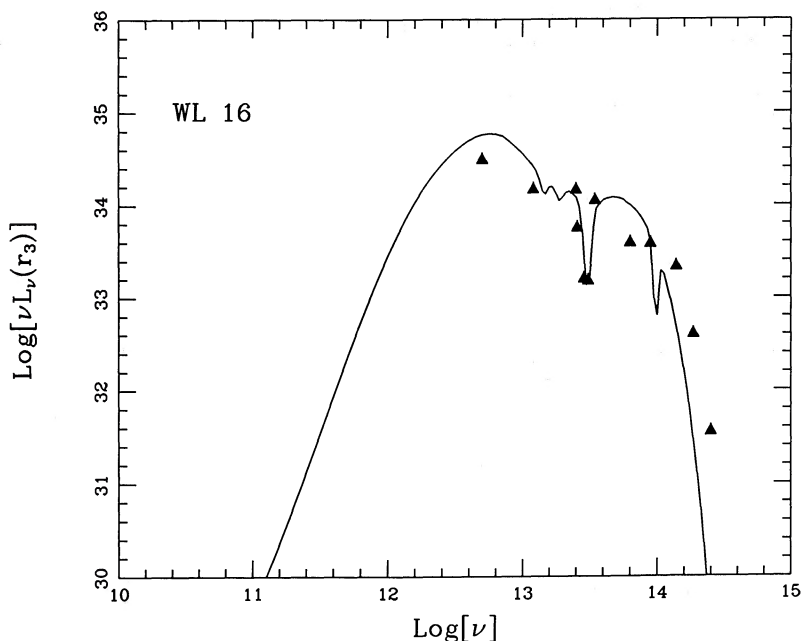


FIG. 1d

FIG. 1.—(c) Haro 6–10 (Taurus): data taken from Myers *et al.* (1986); theoretical curves assume  $a = 0.20 \text{ km s}^{-1}$ ,  $M = 0.5 M_{\odot}$  and  $\Omega = 2 \times 10^{-14} \text{ rad s}^{-1}$ . We have assumed pole-on viewing ( $\theta = 0$ ) based on the location of the infrared source with respect to its associated Herbig-Haro object. The  $U$ ,  $V$ , and  $R$  points (open circles) are probably badly contaminated by scattering. The solid curve makes no correction for this effect; the dashed-dotted curve, the maximum possible correction; and the dashed curve, the “geometric mean” (see Appendix). (d) WL 16 (Ophiuchus): data taken from Wilking and Lada (1983), LW, and Young, Lada, and Wilking (1986); theoretical model assumes  $a = 0.35 \text{ km s}^{-1}$ ,  $M = 0.5 M_{\odot}$ , and  $\Omega = 5 \times 10^{-13} \text{ rad s}^{-1}$ .

#### b) 04016+2610

The Taurus source 04016+2610 has evidence for a weak bipolar flow, and it is intermediate in luminosity between 04365+2535 and Haro 6–10. If we use  $a = 0.20 \text{ km s}^{-1}$  and  $M = 0.4 M_{\odot}$ , we find that a choice  $\Omega = 2 \times 10^{-14} \text{ rad s}^{-1}$ , the value appropriate for Haro 6–10, yields a  $10 \mu\text{m}$  silicate absorption feature of about the right depth (see Fig. 1b). The

spectrum has broadened now to include significant transmission of radiation at frequencies greater than  $10^{14} \text{ Hz}$  ( $\lambda < 3 \mu\text{m}$ ), where there is a systematic departure of the data points from the theoretical curve. This is a typical shortcoming of the protostellar models of AS. We believe that the problem arises from the neglect of the effects of scattering (see Appendix); however, the case cannot be made very strongly here since larger departures (in terms of differential energy content) occur

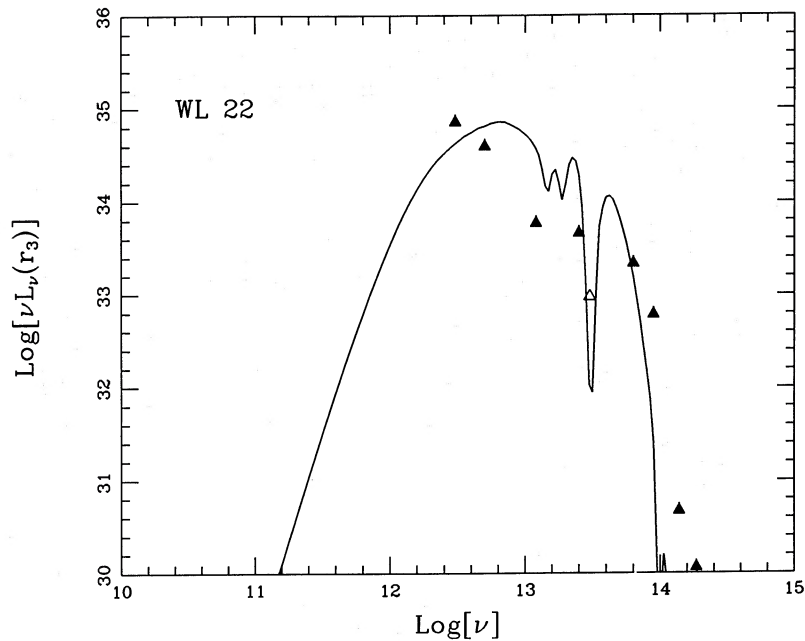


FIG. 1e

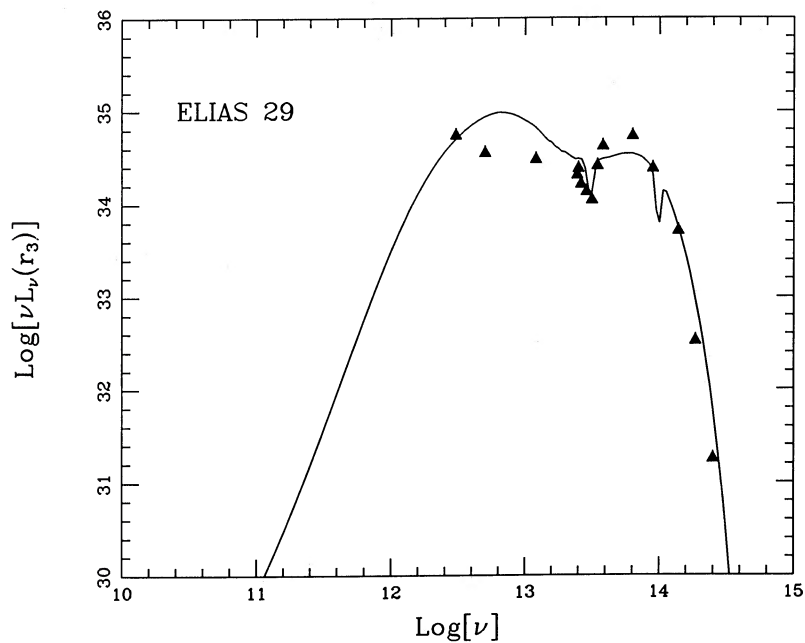


FIG. 1f

FIG. 1.—(e) WL 22 (Ophiuchus): data taken from LW and Young, Lada, and Wilking (1986); theoretical model assumes  $a = 0.35 \text{ km s}^{-1}$ ,  $M = 0.75 M_{\odot}$ , and  $\Omega = 10^{-13} \text{ rad s}^{-1}$ . The open triangle is a broad-band measurement and, therefore, does not give a true indication of the depth of the  $10 \mu\text{m}$  silicate feature. (f) Elias 29 (Ophiuchus): data taken from Elias (1978*a*) and Young, Lada, and Wilking (1986); theoretical model assumes  $a = 0.35 \text{ km s}^{-1}$ ,  $M = 1.0 M_{\odot}$ , and  $\Omega = 2 \times 10^{-13} \text{ rad s}^{-1}$ .

in the frequency range  $10^{12.5} \text{ Hz} < \nu < 10^{13.5} \text{ Hz}$  where scattering is totally negligible. In any case, within the context of our picture of an evolutionary sequence, we envision 04016+2610 as having begun to reverse the infall by pushing out a stellar wind in the polar regions (see Fig. 4 of Shu, Lizano, and Adams 1986).

#### c) Haro 6–10

Although the infrared source Haro 6–10 (in Taurus) has been discussed previously by AS, we include the extension of

the envelope density profile given by equation (8) and calculate a new theoretical model of its spectrum as shown in Figure 1c. Haro 6–10 is associated with a Herbig-Haro object, indicating that it probably has a fairly well developed outflow. Since the H-H object sits almost atop the infrared source (Elias 1978*b*), we adopt a viewing angle  $\theta = 0^{\circ}$  instead of the noncommittal  $45^{\circ}$  chosen for most of our modeled sources. The central source is still highly obscured despite our having such a favorable view, suggesting that either the opening angle of the outflow is fairly narrow or the jet emerging from the poles is not perfectly

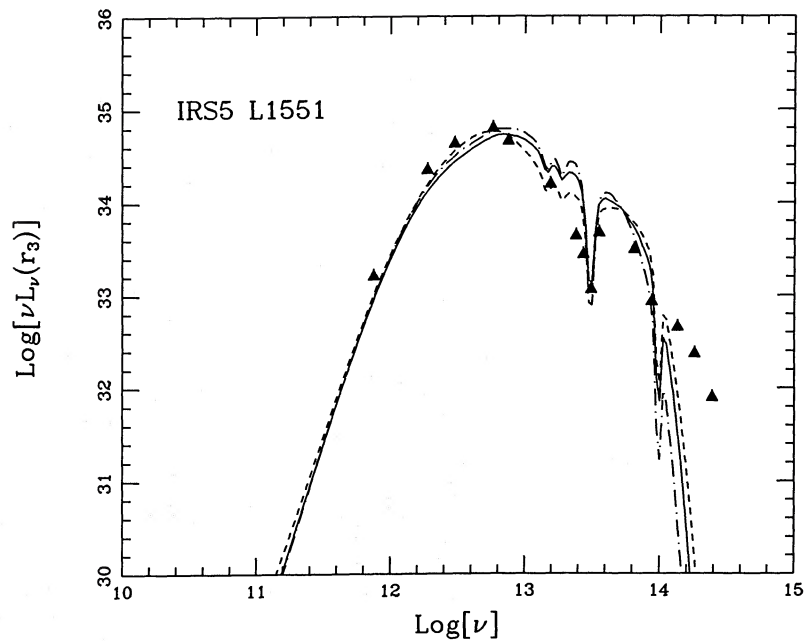


FIG. 1g

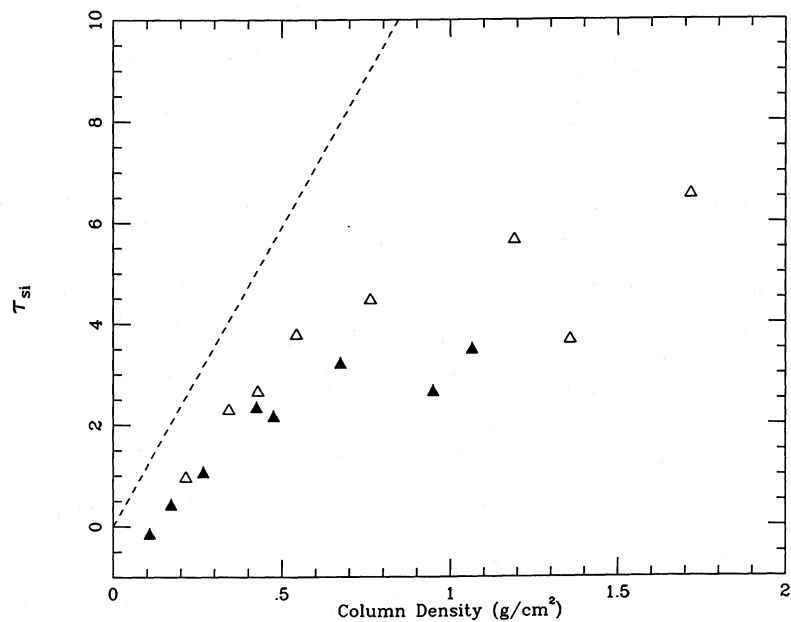


FIG. 1h

FIG. 1.—(g) IRS 5 L1551 (Taurus): data from Cohen and Schwartz (1983), Cohen *et al.* (1984), and Davidson and Jaffe (1984); the theoretical model corresponding to the dashed curve assumes  $a = 0.35 \text{ km s}^{-1}$ ,  $M = 0.5 M_{\odot}$ , and  $\Omega = 5 \times 10^{-13} \text{ rad s}^{-1}$ ; that of the dashed-dotted curve, to  $a = 0.325 \text{ km s}^{-1}$ ,  $M = 0.675 M_{\odot}$ , and  $\Omega = 1 \times 10^{-13} \text{ rad s}^{-1}$ ; and that of the solid curve to  $a = 0.35 \text{ km s}^{-1}$ ,  $M = 1.0 M_{\odot}$ , and  $\Omega = 1 \times 10^{-13} \text{ rad s}^{-1}$  with  $(\eta_*, \eta_D) = (1.0, 0.5)$  instead of  $(0.5, 1.0)$ . In all three models, we have assumed a viewing angle  $\theta = 70^\circ$  on the basis of the ratio of radial and tangential velocities of the Herbig-Haro objects associated with this source (Strom, Grasdalen, and Strom 1974; Cudworth and Herbig 1979). (h) Plot of the silicate absorption depth  $\tau_{\text{si}}$  (for a viewing angle  $\theta = 45^\circ$ ) vs. the (spherically averaged) mass column density  $3.5CR_c^{-1/2}$  to the central source. The filled triangles refer to an effective sound speed of  $a = 0.2 \text{ km s}^{-1}$ ; the open triangles, to  $a = 0.35 \text{ km s}^{-1}$ . The straight line gives the relation that would apply if all of the absorbing dust were in the foreground, i.e., of interstellar rather than circumstellar origin.

straight. If we ignore the effects of the jet, we can model the source as a pure inflow source. Adopting the values  $a = 0.20$  km s<sup>-1</sup> and  $M = 0.5 M_{\odot}$ , we fit the spectrum with  $\Omega = 2 \times 10^{-14}$  rad s<sup>-1</sup>. The emergent spectral energy distribution has more radiation longward of  $\sim 60 \mu\text{m}$  than the models of AS because of the inclusion of emission from larger radii; however, the effect is small, and the derived protostellar parameters are in good agreement with those obtained previously. Notice that the fit of the solid curve to the data is almost perfect, except for a deviation for  $\nu > 10^{14}$  Hz which systematically increases for increasing frequency. This trend is symptomatic of the effects of scattering. Indeed, because the extinction by interstellar dust at visual wavelengths is composed almost equally of scattering and absorption, models which attribute the extinction all to true absorption will severely underestimate the integrated optical light that can escape from deeply embedded sources (Jones 1973). A simple prescription can be derived for placing an upper bound on this effect. This upper bound, which assumes complete forward scattering by the dust particles, is shown as the dashed-dotted curve in Figure 1c; the dashed curve shows a more realistic "geometric mean" between making no correction (*solid curve*) and the maximum possible (see Appendix for details). An angular phase function corresponding to isotropic scattering would probably yield a result similar to that shown for the geometric-mean correction. Scattering has very little direct effect on radiation with frequencies less than  $10^{14}$  Hz; however, there is a slight indirect effect on the pattern of thermal re-emission by the dust envelope because of the changed distribution of heating by optical and near-infrared photons. As a final comment, we note that red and near-infrared photographic images of this source are nonstellar (Elias 1978b), a strong confirmation of our claim that the excess light at such frequencies is due to scattered radiation.

#### d) WL 16

We can further test the ideas described in this section by seeing if the choice  $a = 0.35$  km s<sup>-1</sup> gives acceptable fits for the class (a) infrared sources in Ophiuchus. Two candidates, WL 16 and Elias 29, were selected on the basis that they had fairly extensive spectral coverage as well as narrow-band measurements of (deep) silicate absorption features; a third source, WL 22, was chosen, despite the lack of narrow-band measurements at  $10 \mu\text{m}$ , because its very steep spectrum promised to greatly challenge the theory. The observed spectrum of WL 16, shown in Figure 1d, can be fitted with a theoretical curve using  $M = 0.5 M_{\odot}$  and  $\Omega = 5 \times 10^{-13}$  rad s<sup>-1</sup>. Notice that the inferred angular velocity  $\Omega$  is more than an order of magnitude larger than for the three sources modeled in Taurus. The deduced value for  $\Omega$  could be lowered if  $a$  were made smaller (with  $a^2M$  fixed); however, the fits degrade rapidly, e.g.,  $a$  cannot be as small as  $0.2$  km s<sup>-1</sup> (see also the discussion of IRS 5 L1551). As a precautionary note, we remark that the adopted values for  $a$  and  $\Omega$  for WL 16 imply a "turnover radius,"  $a/\Omega = 7 \times 10^{16}$  cm (see Fig. 1 of TSC), which is comparable to the radius  $GM/m_0 a^2$  of the expansion wavefront and less than  $r_3$  ( $2 \times 10^{17}$  cm); thus, the assumption of equation (8) that the density profile follows a  $r^{-2}$  law from the expansion wavefront to the *IRAS* beam size at  $100 \mu\text{m}$  formally breaks down. The breakdown in the dynamical description of the outer regions does not have an easy realistic cure since the transition from conditions appropriate to the core of a molecular cloud to its envelope depends on the detailed nature (magnetic fields, turb-

ulence, rotation, etc.) of the bulk support for the cloud against its self gravity; fortunately, except at the longest wavelengths, these details should not have a large overall effect on the emergent spectral energy distribution. Finally, we note from Figure 1d that the theoretical curve again predicts less near-infrared flux than is actually observed. Again, the disagreement is probably due to scattering. By making small adjustments in  $\Omega$  and by applying the heuristic (geometric mean) correction outlined in the Appendix, it would be possible—as in the case of Haro 6–10—to obtain better fits to the data. However, since the contribution of the near-infrared to the total luminosity is negligible, the correction would be largely cosmetic. With the implicit understanding that this remark applies to all of our protostellar models, we refrain from further discussion of the effects of scattering on the integrated light.

#### e) WL 22

The infrared source WL 22, also in Ophiuchus, turned out to be difficult to explain (as expected). The best theoretical fit to its spectrum that we could find (with an inclination angle  $\theta$  of  $45^\circ$ ) is shown in Figure 1e, which adopts  $a = 0.35$  km s<sup>-1</sup>,  $M = 0.6 M_{\odot}$ , and  $\Omega = 1 \times 10^{-13}$  rad s<sup>-1</sup>. The steep portion of the spectrum between  $\nu = 10^{12.5}$  and  $10^{13}$  Hz, coupled with the plateau at slightly higher frequencies, poses severe modeling problems. One possible interpretation is that two separate sources are responsible for the radiation  $<$  and  $> 10^{13}$  Hz, and that the steep spectrum of the former is associated with a system being viewed nearly equator-on. Such a geometry would lead to a large anomalous extinction as discussed earlier. In addition, a disk viewed nearly edge-on might possess grains with a distribution of sizes much larger than typical of the interstellar medium. For realistic aspect ratios, say, 10:1, there would be a 10% probability of viewing a disk edge-on. Another possibility is that (one of the components of) WL 22 is being partially viewed through the cloud core associated with WL 16 (see Fig. 1 and Table 1 of Young, Lada, and Wilking 1986), so that considerable foreground extinction exists to the source which is not accounted for in the theoretical model. Narrow band measurements of the silicate features at  $10$  and  $20 \mu\text{m}$  (the displayed  $10 \mu\text{m}$  data point is broad band), and the water ice feature at  $3.1 \mu\text{m}$  (notice that it is off-scale in the theoretical model); and spatially resolved maps of the continuum at near-infrared wavelengths and at  $300 \mu\text{m}$  and  $1$  mm would be helpful in deciphering the properties of this object. Given the existing uncertainties, however, the parameters derived for our current model should be regarded as rather tentative.

#### f) Elias 29

Elias 29 is one of the more luminous infrared sources in Ophiuchus. Figure 1f shows the observed spectrum compared with a theoretical model which uses  $a = 0.35$  km s<sup>-1</sup>,  $M = 1.0 M_{\odot}$ , and  $\Omega = 2 \times 10^{-13}$  rad s<sup>-1</sup>. Notice here that the  $60 \mu\text{m}$  and  $25 \mu\text{m}$  data points (from *IRAS*) fall below the theoretical curve; the deficit at  $60 \mu\text{m}$  may be due to the *IRAS* beam size being smaller (at this wavelength) than is appropriate for the adopted value of  $r_3$  in the theoretical models, but this effect should be less at  $25 \mu\text{m}$ . Again, measurements at longer wavelengths would be helpful in deciding whether the theoretical fit has been overly biased by the  $100 \mu\text{m}$  point.

#### g) IRS 5 L1551

Finally, we present models for the well-known infrared source IRS 5 L1551, discovered by Strom, Strom, and Vrba

(1976). Although L1551 is in the Taurus-Auriga complex of dark clouds, we find that a fairly large value of  $a$  is required to explain the spectrum of IRS 5; this can be seen, for example, by noting that the model developed for WL 16 (in Ophiuchus) gives a good fit for IRS 5 L1551, especially if the viewing angle  $\theta$  is taken to be  $70^\circ$  in accordance with the kinematics of the associated Herbig-Haro objects (see dashed curve in Fig. 1g). The deduced similarity of WL 16 and IRS 5 L1551 found subsequent support in measurements made by C. Lada and G. Wolf (unpublished data) which showed weak emission of about the same strength in the 5:4 line of CS toward both sources, indicating that the excitation conditions in the molecular cloud cores associated with the two objects are similar. In particular, since the telescope beam covers the same linear size in both sources, the CS 5:4 measurements suggest that the coefficient in any precollapse power-law distribution of the density, e.g.,  $\rho = a^2/2\pi Gr^2$ , has about the same value, at least in the part of the inner core which is destined to partake in the inflow. It is this coefficient which determines the important parameter  $\dot{M}$  during the main infall phase. Nevertheless, the exact same model constructed for WL 16 cannot apply to IRS 5 L1551 without coming into conflict with certain direct measurements.

From millimeter-wave observations of the 1:0 transition of CS, Kaifu *et al.* (1984) have deduced a rotation rate  $\Omega = 7 \text{ km s}^{-1} \text{ pc}^{-1}$  in a flattened region of major-axis diameter  $\sim 0.1 \text{ pc} \approx 3 \times 10^{17} \text{ cm}$ . Recent remeasurements by Batria and Menten (1985) find a smaller velocity gradient; the newest estimates from observations in  $\text{NH}_3$  (Menten and Walmsley 1985) and CS (W. Batrla 1986, private communication) give  $\Omega \approx 1 \times 10^{-13} \text{ rad s}^{-1}$ . If we adopt such a value (a slightly larger choice would have been better) and if we keep  $(\eta_*, \eta_D)$  equal to (0.5, 1.0), the dashed-dotted curve in Figure 1g shows the best fit to the observed energy distribution that we can find by varying  $a$  and  $M$  in units of  $0.025 \text{ km s}^{-1}$  and  $0.025 M_\odot$ , with  $a^2 M$  fixed to give the right total luminosity. The resulting values are  $a = 0.325 \text{ km s}^{-1}$  and  $M = 0.675 M_\odot$ . From Figure 1g, we infer that a much greater decrease of  $a$  would have degraded the quality of the resultant fit by an intolerable amount. An alternative strategy which works better with  $\Omega$  given as  $1 \times 10^{-13} \text{ rad s}^{-1}$  is to keep  $a = 0.35 \text{ km s}^{-1}$ , adopt  $M = 1.0 M_\odot$  to obtain roughly the same average column density  $3.5CR_c^{-1/2}$  as the two previous models, and change  $(\eta_*, \eta_D)$  to (1.0, 0.5) to obtain the correct bolometric luminosity. Footnote 1 gives a justification why such choices for the dissipation efficiencies might be especially appropriate for a bipolar outflow source; in any case, the resultant fit is shown as the solid curve in Figure 1g.

The values  $a = 0.325$  and  $0.35 \text{ km s}^{-1}$  correspond, respectively, to temperature equivalents of 30 and 35 K. It is of interest to ask whether the implied enhancement compared with the rest of Taurus has a thermal explanation, or, in contrast with the other sources analyzed in this paper, has significant (precollapse) contributions from turbulence and magnetic fields. The existing evidence on this issue is confused. IRS 5 L1551 has the broadest lines in ammonia of all the protostellar cores in Taurus (P. Myers 1986, private communication); however, collapse motions and interactions with the known bipolar flow (Snell, Loren, and Plambeck 1980) may have contributed appreciably to the observed breadth. The rotational temperatures measured in  $\text{NH}_3$  by Menten and Walmsley (1985) are 9–12 K, consistent with the deduction of Sandqvist and Bernes (1980) from analysis of the 2 mm  $\text{H}_2\text{CO}$  emission, that the gas near IRS 5 (region “C” in their model) has only a

slight enhancement of the kinetic temperature above 10 K. This relatively low value of  $T$  contrasts with the 23 K that Sandqvist and Bernes infer for the centers of the two nearby regions (“A” and “B”) of maximum 2 cm  $\text{H}_2\text{CO}$  absorption, as well as with the general elevation of kinetic temperatures in L1551 (in excess of 18 K), obtained by Snell (1981) from his analysis of the line emission of  $^{13}\text{CO}$ . Further examination of the physical state of the gas within  $10^{17} \text{ cm}$  of IRS 5 in molecular lines which are sensitive to temperature variations as well as density variations would be informative.

An issue of considerable current controversy is the interpretation by Kaifu *et al.* (1984) of the presence in L1551 of a large rotating disk. Our models imply that the true disk in this system—one that becomes supported by centrifugal effects after core collapse (see  $R_C$  in Table 1)—is more than two orders of magnitude smaller than the observed CS structure. This suggests that the latter really represents the equatorial remnant (a “toroid” in the language of Torrelles *et al.* 1983) of the original rotating molecular cloud core which gave birth to the embedded infrared source after a bipolar flow had set in and blown away the polar caps (see the discussions by Cassen, Shu, and Terebey 1985 and by Menten and Walmsley 1985).

In any case, it is intriguing to note that we have little difficulty in constructing self-consistent inflow models which yield spectral energy distributions that fit the prototypical bipolar outflow source, IRS 5 L1551. This provides strong support, in our opinion, for the notion that well-collimated sources require a combination of (rotating) inflow and outflow (Shu and Terebey 1984; Cassen, Shu, and Terebey 1985; Shu, Lizano, and Adams 1986).

By observing scattered optical light that has escaped out the polar directions, Mundt *et al.* (1985) have demonstrated that an open channel does exist in L1551 which probably extends close to the photosphere of IRS 5 ( $A_V \approx 1$  mag along the poles). As long as the channel created by the collimated stellar wind does not clear out infalling dust well beyond  $R_C$  in a large fraction of  $4\pi$  sr centered on the star, the infrared source will probably look very much like a pure infall source, as modeled in Figure 1g. VLA observations of a radio continuum jet associated with IRS 5 L1551 (Cohen, Bieging, and Schwartz 1982; Bieging, Cohen, and Schwartz 1984; Snell *et al.* 1985), as well as optical images of an accompanying jet of  $\text{H}\alpha$  emission (Mundt and Fried 1983; Snell *et al.* 1985), show that the high degree of collimation required for the stellar wind inside 10–100 AU is indeed present.

#### h) Correlation between Silicate Depth and Spectral Breadth

As illustrated in Figures 1a–1g, when  $a$  is known and  $\eta_D(1 + \eta_*\eta_D)a^2M$  is determined from the bolometric luminosity  $L$ , a fit for the depth of the  $10 \mu\text{m}$  silicate absorption feature through the variation of  $\Omega$  automatically produces about the right breadth for the spectral energy distributions of the protostellar candidates. The correlation is nonlinear and occurs essentially because of the dependence of both features on the mass column density to the central source. In Figure 1h we plot the depth of the  $10 \mu\text{m}$  silicate absorption feature,

$$\tau_{\text{si}} \equiv \ln(L_{\text{v}}^{\text{continuum}}/L_{\text{v}}^{\text{line center}}), \quad (15)$$

(at a viewing angle  $\theta = 45^\circ$ ) as a function of the average mass column density,  $3.5CR_c^{-1/2}$ , for all the protostellar models which were constructed in connection with the preparation of this paper. Different symbols are used to plot the cases for  $a = 0.2 \text{ km s}^{-1}$  and  $a = 0.35 \text{ km s}^{-1}$ . Also plotted is the

straight line relation that would result if the silicate absorption were all produced by foreground (e.g., interstellar) dust; departures from the straight line relation occur when  $R_C$  lies near or below the radius where the  $10\ \mu\text{m}$  continuum is formed at a (circumstellar) temperature of about 300 K. In particular, notice the zero-point offset of the plotted points which occurs because the circumstellar silicate feature can actually go into emission (negative  $\tau_{\text{si}}$ ) for low values of the column density.

Figure 1h can be potentially used as a statistical check of the theory by observers who have access to large data bases where it would be impractical to try to model the spectral energy distribution of each source in detail. For example, the mass column density can be estimated by dividing the visual opacity (for bare grains) of  $200\ \text{cm}^2\ \text{g}^{-1}$  into a measured value of the extinction  $A_V$  to the central source.<sup>2</sup> Narrow-band observations at  $10\ \mu\text{m}$  would directly yield  $\tau_{\text{si}}$ , and a plot of the latter versus  $A_V$  (or the mass column density) would reveal whether the data point falls within the range indicated by Figure 1h. If so, then one would have an empirical estimate for the combination  $3.5CR_C^{-1/2} \propto a^7/M^2\Omega$ , from which one could, in principle, derive protostellar masses  $M$  if  $a$  and  $\Omega$  (or  $R_C$ ) were known, say, from radio-astronomical measurements. Unfortunately, the sensitive dependence on  $a$  probably renders such an approach impractical except as a crude dynamical check on masses  $M$  which are derived from luminosities  $L$ . (The latter approach suffers from the need to make assumptions concerning the stellar and disk dissipation efficiencies,  $\eta_*$  and  $\eta_D$ .) Clearly, spectroscopic diagnostics of the inflowing velocity field need to be developed if we are to make further progress on this problem.

To close this section we comment that although our fits for class (a) sources as protostars are imperfect, they yield a remarkably close correspondence given the simplicity of the underlying theory and the restrictions that we have placed on the search in parameter space. Of course, we have shown here only that our infall models are sufficient to explain the observations of class (a) sources; we have not demonstrated necessity. The complementary discussion of Myers *et al.* (1986), who do not restrict themselves to dynamically and energetically self-consistent models, come close to demonstrating that ideas like those introduced by Shu (1977), TSC, and AS are indeed necessary. In particular, Myers *et al.* argue convincingly that the density distribution of dust surrounding their protostellar candidates must be centrally concentrated, that the effective cutoff for the "inner radius" of a power-law envelope must exceed the radius of the dust destruction front by a factor like that associated with  $R_C$ , and that a warm, extended, radiating component (i.e., a "disk") is needed to account for the "missing mid-infrared" which results if only a star and circumstellar envelope are included in the model calculation.

### III. T TAURI STARS WITH PASSIVE DISKS

In accordance with the view of star formation espoused above and elsewhere, the infall phase of protostellar evolution ends when the star reverses the infall and becomes optically visible. In such a picture, the newly born star will be surrounded by a dusty gaseous disk which will reprocess stellar

photons according to the heating and shadowing process presented as AS; in addition, there may be *intrinsic* disk luminosity due to viscous accretion (e.g., Lin and Papaloizou 1985). However, even in the absence of disk accretion, AS showed that (in the limit of a large disk radius) an optically thick disk will intercept 25% of the luminosity of the central star and reprocess it into the infrared. The equilibrium temperature of such a disk will have a radial distribution given approximately by  $\sigma T^4 \propto r^{-3}$ . This result can be understood physically by noting that the stellar flux drops as  $r^{-2}$  and there is an additional projection factor of approximately  $R_*/r$  associated with the interception geometry for a spatially flat disk (more accurate formulae are given in AS). Thus, a disk with *no* intrinsic luminosity will radiate with an effective luminosity of  $L_*/4$ . The spectral distribution of this flux will have an approximate power-law behavior in the mid-infrared to near-infrared given by  $\nu L_\nu \propto \nu^{4/3}$ , which mimics the behavior of a Keplerian accretion disk (see Lynden-Bell and Pringle 1974).<sup>3</sup>

The distinction between the two possibilities, then, lies not in the slope of the spectrum in  $\log(\nu)$ - $\log(\nu L_\nu)$  space, but in the intercept: the passive disk model gives the *minimum* infrared emission from an optically thick disk; reprocessing of stellar photons is always present whether accretion also occurs or not. Thus, if the passive model gives the requisite infrared excess, there is no room for much active accretion.

The above argument presupposes that we know the basic properties of the star, in particular, its luminosity  $L_*$  and effective temperature  $T_*$ . In those cases where this information is less secure (e.g., FU Orionis to be discussed later), the argument becomes more complicated. A possible distinction may then lie in the absence or presence of an accretion boundary layer (Lynden-Bell and Pringle 1974; Hartmann and Kenyon 1985). Since T Tauri stars are known observationally to be slow rotators in general (Vogel and Kuhl 1981; Hartmann *et al.* 1986), active accretion from a Keplerian disk should give rise to a boundary layer which radiates as much energy in the ultraviolet as the disk proper radiates in the infrared. Although T Tauri stars do have ultraviolet excesses, the excesses are generally not extreme and have conventionally been associated with active chromospheres (see, e.g., Calvet, Basri, and Kuhl 1984). More study of this phenomenon is needed.

In any case, the shadowing of the star by a passive disk will typically reduce the optical stellar luminosity to  $3L_*/4$  (when viewed from a random direction), and the further attenuation by  $\sim 1$  mag of visual extinction will make the near-infrared luminosity comparable to the remaining stellar luminosity, the typical outcome observed for T Tauri stars (Rydgren, Strom, and Strom 1976; Cohen and Kuhl 1979; LW). Thus, passive or nearly passive disks provide a natural explanation for one type of infrared excess associated with T Tauri stars. The other type, flat spectrum sources which involve spectral indices  $n$  between 0 and  $4/3$  (see Rydgren *et al.* 1984 and Rucinski 1985), may well require active accretion, but perversely, not via a classical *Keplerian* disk! We shall return to a discussion of this second type in § VI; in the present section, we provide quantitative justifications for the assertion that passive disks can explain the infrared excesses associated with T Tauri stars whose spectral indices  $n$  have appreciable positive values.

The energy distributions from a star and disk at distance  $r$

<sup>2</sup> Actually, the estimate is slightly tricky since, as we have emphasized at a number of different points, observations at visual wavelengths need to correct for light returned by scattering to a beam of finite size (see Appendix). Scattering is less of an effect in the near-infrared, but neglect of emission by the disk and by the circumstellar envelope can also lead to underestimates of  $A_V$ .

<sup>3</sup> This mimicry of the spectral behavior of Keplerian accretion disks has been independently noted by Friedjung (1985).

with radii  $R_*$  and  $R_D$  are given by

$$4\pi r^2 F_{\nu}^* = 4\pi^2 R_*^2 B_{\nu}[T_*] g_D(\theta) \exp[-\tau_{\nu}], \quad (16a)$$

$$4\pi r^2 F_{\nu}^D = 2 \int_{R_*}^{R_D} 2\pi \varpi d\varpi \pi B_{\nu}[T_D(\varpi)] (2 \cos \theta) g_*(\theta) \exp[-\tau_{\nu}], \quad (16b)$$

where  $g_D(\theta)$  and  $g_*(\theta)$  are the functions defined in the Appendix of AS which take into account the mutual shadowing of the star and disk. Here we have also included the attenuation due to interstellar or circumstellar dust with the optical depth given in terms of the visual extinction by

$$\tau_{\nu} = \kappa_{\nu} A_V / \kappa_c, \quad (17)$$

where  $\kappa_c$  is a constant (taken here, for simplicity, to be  $200 \text{ cm}^2 \text{ g}^{-1}$ ) and where  $\kappa_{\nu}$  is the frequency-dependent dust-grain opacity (taken from the opacity profile in AS which is, in turn, based on the calculations of Draine and Lee 1984).

Once the characteristics of the star and disk are determined, equations (16) and (17) completely specify the spectral energy distribution. We use observations to determine the total luminosity  $L$  and the visual extinction  $A_V$ . The sources that we consider here are of known spectral type, and hence have a corresponding surface temperature  $T_*$ , allowing the stellar radius to be obtained through

$$R_* = (L/4\pi\sigma T_*^4)^{1/2}. \quad (18)$$

Since the heating of the star by the disk is usually a small effect, equation (18) involves little error. As discussed in AS, the spectral energy distribution is not very sensitive to the disk radius; hence, we use a single characteristic value,  $R_D = 10^{15} \text{ cm}$ , throughout the present work. As argued above, the temperature distribution in the disk can be taken to have the power-law distribution,

$$T_D(\varpi) = T_{D*} (\varpi/R_*)^{-3/4}, \quad (19)$$

with the coefficient  $T_{D*}$  calculated in accordance with the formula (A19b) of AS when the intrinsic luminosity  $L_D$  of the disk is set equal to zero (except for one model of FU Orionis).

#### a) SR 9

Using the formulation described above, we can calculate the spectral energy distribution for specific sources which have been selected for the steepness of their near-infrared spectra. Figure 2a shows the observed spectrum of SR 9 along with a theoretical model. Since this source is a K5 star (Rydgren, Strom, and Strom 1976), we use a surface temperature of 4000 K. The visual extinction is taken to be 1.0 mag (Cohen and Kuhl 1979). We find that a luminosity of  $3.0 L_{\odot}$  fits the observed energy distribution better than the  $4 L_{\odot}$  quoted by Cohen and Kuhl. In the theoretical model we have taken pains to count only the primary sources of photons in a geometry where the integral of  $4\pi r^2 F_{\nu}$  over all frequencies at a given  $\theta$  can differ from the actual bolometric luminosity  $L$  by 25% or more (see Appendix of AS). Also shown in the figure is a reddened blackbody corresponding to the star with no disk; notice that the absolute level of the infrared excess is well represented by the simple model of a passive nebular disk.

#### b) SU Aurigae

The observed spectrum of SU Aur and its theoretical counterpart are shown in Figure 2b. Here, the star is a G2 III

star with a corresponding surface temperature of 5800 K (Cohen and Kuhl 1979). The total luminosity of the source is given as  $15 L_{\odot}$  with a visual extinction of 1.5 mag. Again, the presence of a disk is necessary to account for the near-infrared excess. Notice that at wavelengths longer than  $10 \mu\text{m}$ , the data depart from the simple theoretical curve, suggesting that an additional element should be included in the calculation; this issue is addressed in the next section where we incorporate a residual dust envelope.

### IV. T TAURI STARS WITH RESIDUAL DUST ENVELOPES

#### a) Residual Circumstellar Dust Envelope

Since T Tauri stars generally show the effects of extinction, and since we mostly view these systems in directions well off the disk plane, there must be dusty circumstellar material surrounding these objects in a more-or-less extended fashion. The absorption of photons by this dust envelope must be accompanied by thermal reemission, with the corresponding spectral energy distribution determined by the exact geometry of the dust shell. From the examples considered in the previous section, it would not be unreasonable to guess that a visual extinction  $A_V$  of 1 mag or less generally corresponds to dust which lies at fairly large distances from the star; such grains will reproduce radiation into the far-infrared, where measurements are generally not available or are easily confused with the background. However, larger values of  $A_V$  could arise from leftover matter (residual infall?) from the collapse of the original molecular cloud cores; material within  $10^{15}$ – $10^{16} \text{ cm}$  of a star will reprocess stellar radiation into the mid-infrared and should be included in the calculation. Toward this end, we now develop a model for a circumstellar dust shell that attenuates and reemits stellar (and disk) photons.

We begin by considering a piece (or pieces) of a spherical envelope with covering fraction  $f$  that is optically thin to its own thermal photons so that the additional spectral energy  $\mathcal{L}_{\nu}$  from dust emission is given by

$$\mathcal{L}_{\nu} = f \int_{r_0}^{\infty} \rho \kappa_{\nu} 4\pi B_{\nu}(T) 4\pi r^2 dr, \quad (20)$$

where  $r_0$  is the inner radius of the dust envelope and the outer radius of the envelope has been extended to infinity. For  $r > r_0$ , we can parameterize the density distribution, in the directions included in the covering fraction  $f$ , as a fraction  $\gamma$  of the density of the original molecular cloud core from which the star and disk formed (see Shu 1977):

$$\rho = \frac{\gamma a^2}{2\pi G} r^{-2}. \quad (21)$$

The factor  $\gamma$  can be interpreted as a depletion of the initial density profile because of the infall during the earlier protostellar phase. In this interpretation, the circumstellar dust envelope arises from residual infall in those directions which have not been completely swept clean by the stellar wind. In any case, our adopted density profile has two parameters,  $r_0$  and  $\gamma$ . One of these (we choose  $r_0$ ) can be specified by requiring the visual extinction calculated using equation (21) to agree with the observed value:

$$r_0 = \frac{\gamma \kappa_c a^2}{2\pi G A_V}, \quad (22)$$

assuming that the line of sight is included in the covering fraction  $f$ .

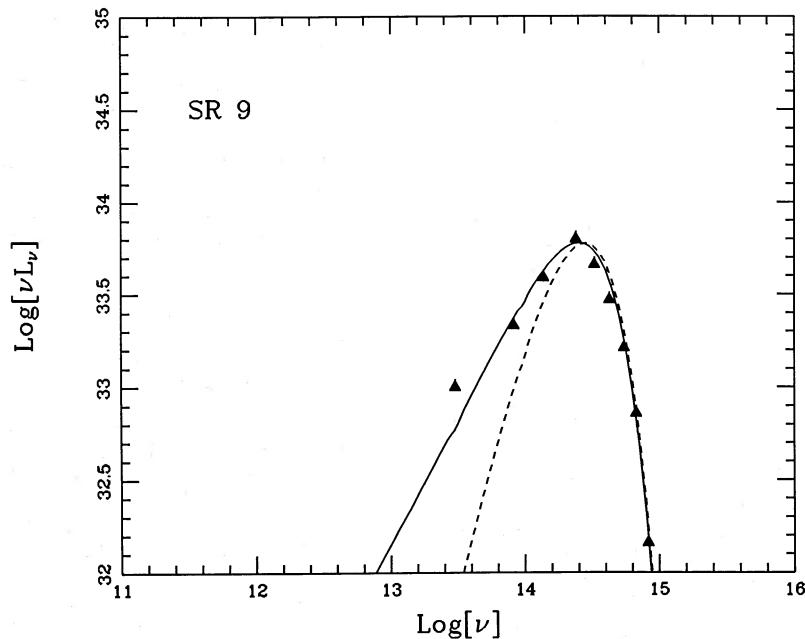


FIG. 2a

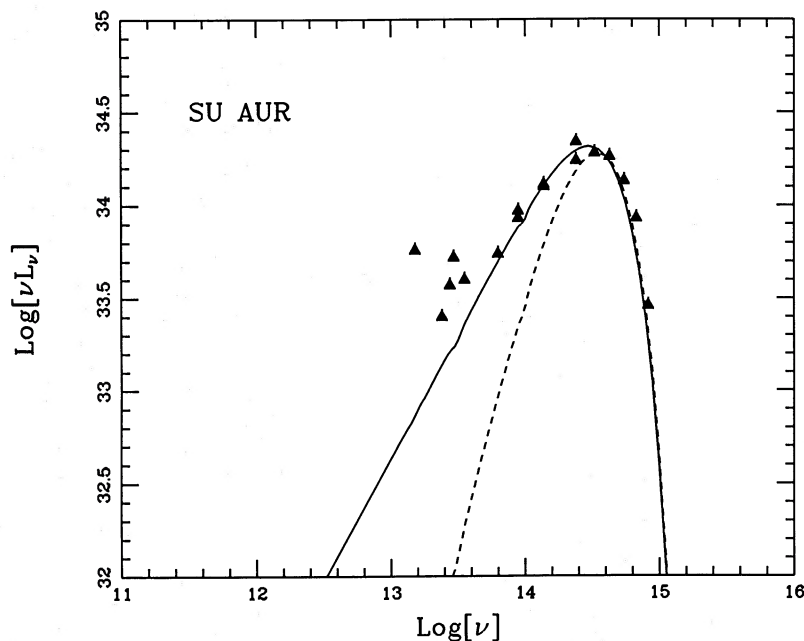


FIG. 2b

FIG. 2.—Theoretical and observed spectra of T Tauri stars with infrared excesses. The theoretical models consist of a star with an optically thick disk and an overall attenuation factor. A reddened blackbody (*dashed line*) is shown for comparison. (a) SR 9 (Ophiuchus): data from Chini (1981) and LW; theoretical model assumes  $L = 3.0 L_{\odot}$ ,  $A_V = 1.0$  mag, and  $T_{*} = 4000$  K. (b) SU AUR (Taurus): data from Rydgren, Strom, and Strom (1976) and Mendoza (1966, 1968); theoretical models assumes  $L = 15.0 L_{\odot}$ ,  $A_V = 1.5$  mag, and  $T_{*} = 5800$  K.

For a given  $\gamma$ , it is possible to determine the dust temperature profile using a self-consistent numerical technique similar to that developed in AS; however, our experience shows that an adequate approximation results by adopting the optically thin solution,

$$T = T_0(r_0/r)^{1/3}. \quad (23)$$

If we now integrate equation (20) over all frequencies, the total

luminosity from the dust envelope can be expressed as

$$\mathcal{L} = f\gamma 8\sigma a^2 B T_0^6 r_0/G, \quad (24)$$

where we have assumed that the Planck mean opacity at low temperatures can be approximated as

$$\kappa_P = B T^2. \quad (25)$$

Here, the constant  $B$  is taken to be  $2.38 \times 10^{-4} \text{ cm}^2 \text{ g}^{-1} \text{ K}^{-2}$ , a value consistent with Figure 2 of AS.

On the other hand, conservation of energy implies that

$$\mathcal{L} = f \left[ L - \int_0^{\infty} L_{\nu}^c \exp(-\tau_{\nu}) d\nu \right], \quad (26)$$

where  $\tau_{\nu} = \kappa_{\nu} A_{\nu}/\kappa_c$  is the optical depth to the center along the line of sight through the dust envelope at the frequency  $\nu$ . With  $\mathcal{L}$  constrained by equation (26), equations (22) and (24) can now be used to calculate  $T_0$ :

$$T_0 = (\pi G^2 A_{\nu} \mathcal{L} / 4\sigma B \kappa_c a^4 f \gamma^2)^{1/6}. \quad (27)$$

The substitution of constraint (26) recovers the physically reasonable expectation that  $T_0$  is independent of  $f$ . We assume that  $f$  is usually of order unity when  $A_{\nu}$  is considerable. Thus, we are left with effectively only a single undetermined (nondimensional) parameter:  $\gamma$ . Its value, which determines both the (average) density depletion factor and the radius  $r_0$  of the inner dust envelope, can be chosen to give the correct frequency location for the observed peak of mid-infrared and far-infrared radiation from the dust envelope.

#### b) VSSG 23

With the procedure outlined above, we find that the "double-humped" spectrum of VSSG 23 (Vrba *et al.* 1975) can be fitted quite well. Figure 3 shows the observed spectral energy distribution with a theoretical model calculated according our stated formalism. This object has been classified as a K0 star (Chini 1981), so we have assumed a stellar temperature of 4500 K. The luminosity ( $L = 6.0 L_{\odot}$ ), the isothermal sound speed ( $a = 0.35 \text{ km s}^{-1}$ ), and the visual extinction ( $A_{\nu} = 5.0 \text{ mag}$ ) of the theoretical model have been chosen to be consistent with the values cited in the literature. We set the covering fraction  $f$  equal to 1 and find that the parameter  $\gamma$  must have a value of 0.01 to match the observed location of the low-frequency radiation peak; the resulting height and breadth of the spectrum are then natural consequences of the basic model.

It is interesting to note that the resulting value of  $r_0$ , 80 AU, is typical of the centrifugal radii  $R_c$  of the protostellar models in Ophiuchus (Table 1), and that density depletion factors of roughly  $10^{-2}$  due to infall are typical at late times for such radii (see curve 8 of Fig. 3a in Shu 1977 and compare it with the inward extrapolation of the dashed line). These two coincidences reinforce our interpretation of the dust envelope as residual infall (probably in an equatorial belt of the system because the basic model envisages outflow to open progressively from the polar axes). We emphasize, however, that the only conclusion justified from an examination of the infrared continuum alone is that in VSSG 23 there must be an extended distribution of dust located at a characteristic distance of about  $10^{15} \text{ cm}$  from the star. The decision to model this envelope as being centrally condensed, rather than a uniform shell, derives from the dynamical intuition that dust not confined to the same flat plane as the disk which is responsible for the near-infrared emission must be infalling rather than static.

#### V. FU ORIONIS

As a further application of the model developed in the previous sections, we consider the famous outburst source FU Orionis. If we use the technique of § III and assume that all of the (intrinsic) luminosity of this source comes from a star with surface temperature  $T_* = 7000 \text{ K}$ , we find that a stellar luminosity  $400 L_{\odot}$  with  $A_{\nu} = 2.4$  is required in order to reproduce the observed spectrum; the result is shown as the solid curve in Figure 4a. Inclusion of the emission from a circumstellar dust shell (see § IV) yields a somewhat better fit to the observed data, the dashed curve in Figure 4a. Again, to obtain the correct location for the peak of the low-frequency radiation, the parameter  $\gamma$  must have a value of 0.01. However, in order to obtain the correct height, the circumstellar envelope must have a covering fraction of  $f = 0.1$ . This conclusion is clearly very sensitive to the assumption that the column density of dust

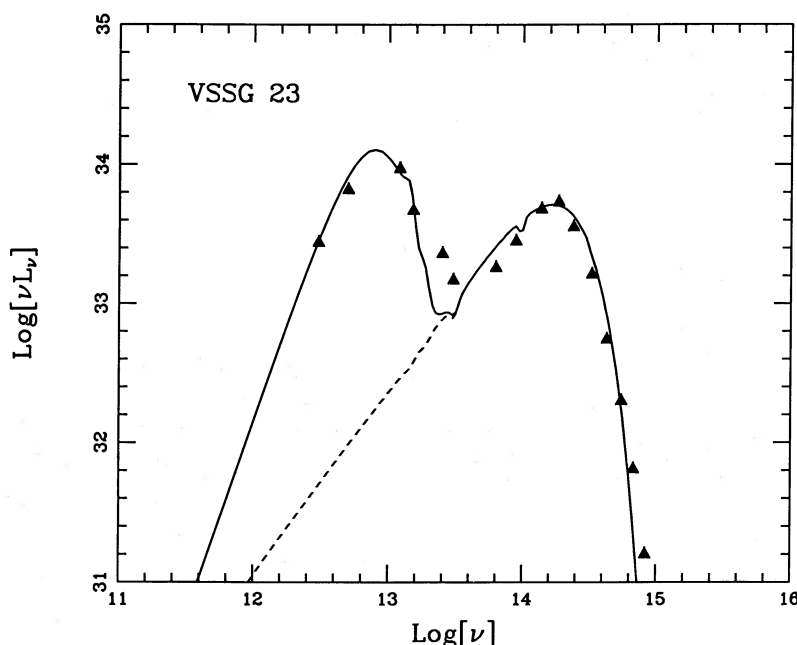


FIG. 3.—VSSG 23 (Ophiuchus): data from Chini (1981), Wilking and Lada (1983), and LW; the theoretical model includes the emission from a dust shell, optically thin in the infrared, with a unit covering fraction surrounding the central star and disk. The model assumes  $L = 6.0 L_{\odot}$ ,  $A_{\nu} = 5.0 \text{ mag}$ , and  $T_* = 4500 \text{ K}$ . The dashed line shows the spectrum with the contribution from the dust envelope removed.

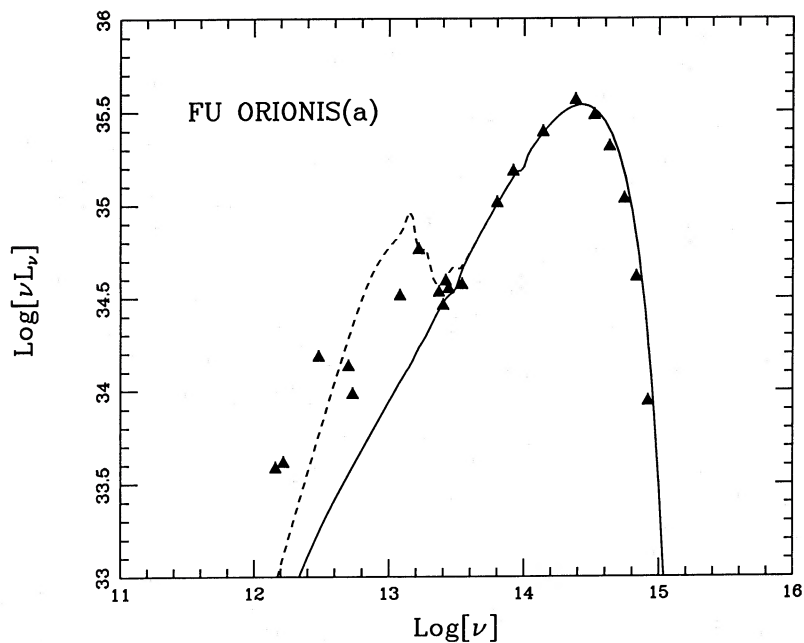


FIG. 4a

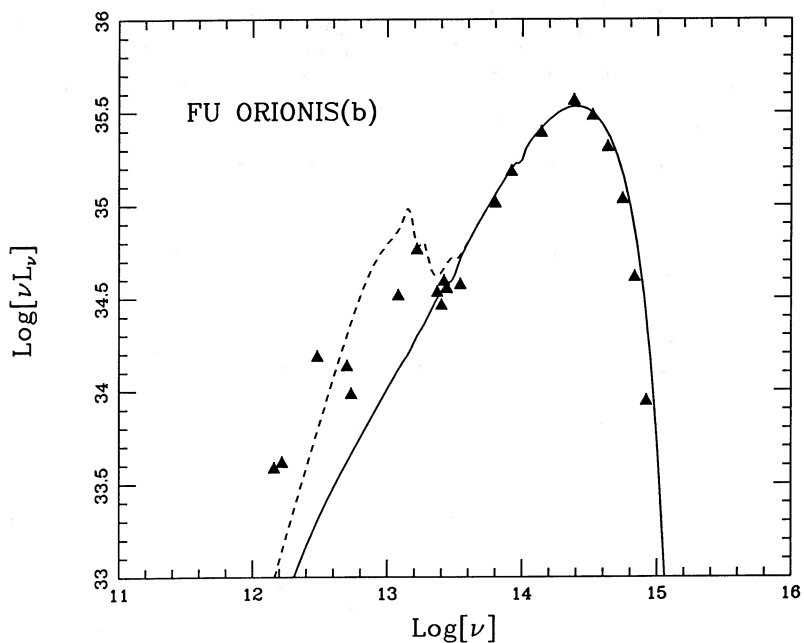


FIG. 4b

FIG. 4.—FU Orionis (Orion, distance = 400 pc): data from Smith *et al.* (1982); (a) the disk is passive and only radiates photons intercepted from the (outbursting) star with temperature  $T_* = 7000$  K; (b) the disk is active and provides all of the outburst luminosity in an accretion process through a Keplerian disk. The dashed curve in both figures shows the emission from a surrounding dust shell with a covering fraction equal to 0.1. Both cases require  $L = 400.0 L_\odot$  and  $A_V = 2.4$  mag.

along the line of sight is typical of the portion of the sky which contains circumstellar matter. There exists some observational evidence which favors the view that the circumstellar material around FU Orionis is patchy or forms an incomplete shell (Smith *et al.* 1982).

The spectrum of FU Orionis can also be explained if we make the assumption that *all* of the luminosity of this source arises from a Keplerian disk, presumably through some accretion process involving a disk instability. (In this picture, the

star radiates due to heating by the disk in accordance with the prescription outlined in the Appendix of AS.) If we assume an intrinsic disk luminosity  $L_D$  of  $400 L_\odot$  (where the intrinsic stellar luminosity  $L_*$  has been set equal to zero for simplicity) and  $A_V = 2.4$  mag, we obtain an almost identical fit to the observed spectrum, as shown by the solid curve in Figure 4b. Also shown (*dashed curve*) is a theoretical model including emission from a circumstellar dust envelope using the same parameters as in the stellar outburst model.

Thus, the spectrum of FU Orionis can be explained either in terms of an outbursting star with a passive disk that reprocesses stellar photons, or as an active (Keplerian) disk undergoing a burst of accretion which also happens to heat the star (about 7.6% of the disk luminosity is reprocessed by the star). A detailed analysis of the line spectrum is probably needed to distinguish between these two extreme possibilities; however, severe chromospheric effects in T Tauri-like stars (Calvet, Basri, and Kuhi 1984) may complicate any interpretation. Polarization measurements along with scattering calculations may provide another important diagnostic. Although the models of the continuum radiation presented here do not resolve the controversy concerning the ultimate outburst mechanism for the FU Orionis phenomenon, they do provide strong evidence for the existence of a disk in the prototype of such systems.

## VI. DISCUSSION

We have presented an evolutionary sequence for the emergent spectral energy distributions of (low-mass) young stellar objects. The first member of this sequence corresponds to a true protostar, an object characterized by a central star with an infalling envelope of gas and dust. We have shown that the protostellar models of AS explain the observed infrared sources with steep negative indices in Taurus and Ophiuchus. In fitting these spectra, we have used the measured cloud temperature and total system luminosity to determine the isothermal sound speed  $a$  and the mass  $M$ , respectively, leaving a single parameter, the angular velocity  $\Omega$ , with which to match the data. In all of the studied cases, the derived angular velocities are physically reasonable, lying in the range  $2 \times 10^{-14}$  to  $5 \times 10^{-13}$  rad s $^{-1}$ . In addition, the angular rotation rate  $\Omega$  appears to be correlated with the effective sound speed  $a$ : the value of  $\Omega$  is found to increase with increasing  $a$ , an effect also seen in the observational data of Myers (1986). Shu, Lizano, and Adams (1986) have speculated that the temperatures and angular rotation velocities are higher in Ophiuchus than in Taurus because the former represents a supercritical region where the self-gravity of a large dense core has overwhelmed the magnetic support. This gives rise to relatively rapid ambipolar diffusion (and, therefore, direct gas heating), efficient star formation, and decreased magnetic braking.

The pure infall phase is followed by a bipolar flow phase, in which inflow and outflow occur simultaneously. However, as long as the solid angles subtended by the outflowing jets remain small, the emergent spectra of such sources should be essentially indistinguishable from those of true protostars, unless the observational line of sight happens to coincide with the axis of a jet (see the discussion concerning IRS 5 L1551).

When the outflow widens to encompass a substantial fraction of the celestial sphere centered on the star, the emergent spectra become that of the next class of sources, pre-main-sequence stars with infrared excesses. We have shown that some of these sources can be understood as T Tauri stars with surrounding nebular disks, where the disks have no intrinsic luminosity but reprocess stellar photons to produce the observed infrared emission. There may also be cases where the nebular disk does have intrinsic luminosity. For example, as mentioned earlier, there are many objects observed which have flat infrared spectra in the  $\log(\nu)$ - $\log(\nu L_\nu)$  plane. One possible explanation for these sources is that they have optically thick disks with temperature distributions which satisfy  $T \propto \varpi^{-1/2}$ , rather than the  $T \propto \varpi^{-3/4}$  law that seems to characterize opti-

cally thick but spatially thin disks which merely reprocess stellar photons (e.g., SR 9).

A disk temperature distribution that departs from  $T \propto \varpi^{-3/4}$  might arise for a number of reasons: (1) radiative transfer effects, (2) extreme geometric flaring or warping, or (3) disk accretion in a non-Keplerian velocity field. The last possibility was suggested to us by Peter Strittmatter and Roger Thompson (1986, private communication) and is, in our opinion, the most exciting possibility from a physical point of view. Non-Keplerian rotation would imply that the nebular disks around some young stellar objects are massive enough to be self-gravitating. Consider steady state accretion at a constant rate  $\dot{M}_a$  to take place locally because of the action of a torque  $\mathcal{T}$  exerted by material inside a circle of radius  $\varpi$  on the matter outside it in a disk which rotates at angular speed  $\Omega$ . The rate of energy dissipated (stress  $\times$  strain) through the action of this torque in an annular region should be balanced by radiation through the top and bottom surfaces of the annulus (cf. Lynden-Bell and Pringle 1974):

$$-\mathcal{T} d\Omega = 2 \cdot \sigma T^4 \cdot 2\pi\varpi d\varpi. \quad (28)$$

Accretion occurs because the same torque  $\mathcal{T}$  transfers angular momentum (outward if  $d\Omega/d\varpi < 0$ ) at a rate equal to  $\dot{M}_a \varpi^2 \Omega$ :

$$\mathcal{T} = \dot{M}_a \varpi^2 \Omega. \quad (29)$$

The substitution of equation (29) into equation (28) yields an effective temperature for the disk locally given by

$$T = \left( -\frac{\dot{M}_a}{4\pi\sigma} \varpi \Omega \frac{d\Omega}{d\varpi} \right)^{1/4}. \quad (30)$$

Equation (30) yields  $T \propto \varpi^{-3/4}$  for a Keplerian disk,  $\Omega \propto \varpi^{-3/2}$ , and  $T \propto \varpi^{-1/2}$  for a Mestelian disk,  $\Omega \propto \varpi^{-1}$ . Notice that the derivation of the formula (30) depends on the notion that the dissipative disk torque  $\mathcal{T}$  acts on an axisymmetric system but is otherwise insensitive to the details of its origin; it could arise from viscous, magnetic, or gravitational effects (see, e.g., the discussion of Cassen, Shu, and Terebey 1985).

Rotation curves which are flatter than Keplerian are, however, usually associated with extended mass distributions (e.g., in a galaxy). Through infall, protostellar disks can acquire masses comparable to those of their central stars if the disk processing efficiency  $\eta_D$  is of order  $\frac{1}{2}$  or less; such massive disks might well exist around revealed T Tauri stars whose ages are not much advanced beyond the infall phase. From this point of view, it is intriguing that flat-spectrum sources seem to correspond to those stars which show the greatest emission-line activity (see, for example, Fig. 7 of Rydgren, Strom, and Strom 1976). It is also intriguing that T Tauri itself is a flat spectrum source (Rydgren, Strom, and Strom 1976) and has a companion at a distance of about 100 AU (Dyck, Simon, and Zuckerman 1982; Schwartz *et al.* 1984), perhaps indicating that such binaries form from massive disks.<sup>4</sup> A disk origin, rather than independent condensation, for binaries with periods shorter than  $\sim 10^2$  yr may explain the striking fact of their non-random mass ratios (see Abt 1983).

The assumption of axial symmetry in the derivation of equa-

<sup>4</sup> Our identification of T Tauri's companion as a star, rather than, e.g., a giant protoplanet with starlike luminosities (Hanson, Jones, and Lin 1983), relies on the interpretation of the mid-infrared and far-infrared radiation coming from a (non-Keplerian) disk rather than from the companion.

tion (30) is somewhat worrisome inasmuch as the largest known sources of torques in angularly resolved astrophysical disks—spiral galaxies and Saturn's rings—are, in fact, associated with nonaxisymmetric disturbances. Thus, it is significant that there is a more robust argument for massive disks than the interpretation of the detailed shape of the infrared spectra. This argument begins by noting that flat-spectrum T Tauri stars have infrared excesses above the fractional value ( $\frac{1}{4}$ ) which can be ascribed to simple reprocessing of stellar light in passive disks. There must be an additional source of energy for heating such disks, and the most likely candidate is accretion of some sort, axisymmetric or nonaxisymmetric, onto the T Tauri star itself or one or more companions. If the depth of the associated gravitational potential is starlike, then the total accretion rate must be  $\sim 10^{-6} M_{\odot} \text{ yr}^{-1}$  in order to explain the observed excess infrared luminosity (Rucinski 1985 quotes  $10^{-6}$  to  $10^{-5} M_{\odot} \text{ yr}^{-1}$ ; the requirements are more severe with planetary bodies). But the majority of T Tauri stars have such excesses, and their lifetimes are conventionally estimated to be of order  $10^5$ – $10^6$  yr (e.g., Cohen and Kuhi 1979). Thus, the reservoirs of material for accretion in the disks must often be of order 0.1–1  $M_{\odot}$ , i.e., comparable to the masses of the T Tauri stars themselves. A disk mass in the lower range of this order has been deduced (Beckwith *et al.* 1986; Sargent and Beckwith 1986) for HL Tau, which is a flat spectrum T Tauri star with a rising hump toward the far infrared.

In addition to the issue of low-mass and high-mass disks, class (b) of pre-main-sequence systems can be further divided into two subcategories—those with and without circumstellar dust envelopes. The subclass with surrounding dust shells, which probably arise from residual infall, have larger visual extinctions and may represent a younger evolutionary phase. This interpretation is consistent with the finding of Cohen (1986) that the ratio of far-infrared luminosity to stellar luminosity *decreases* as T Tauri stars evolve toward the main sequence from the stellar “birthline.” Since the residual infall is probably highly anisotropic, the simple quasi-spherical modeling given in this paper is somewhat idealistic and should be interpreted cautiously. However, unlike the disk emission, the thermal emission from the residual envelope is likely to occur under optically thin conditions. Hence, the details of the treatment should not be important as long as the total mass of the dust and its temperature profile have been properly taken into account. It is, therefore, suggestive that the one vital free parameter,  $\gamma$ , in this procedure gives a density depletion factor (see eq. [21]) and an inner radius  $r_0$  (see eq. [22]) which are

consistent with the dynamics of the adopted rotating infall model for the earlier protostellar phase.

Following the removal of the residual dust envelopes and the nebular disks (or their incorporation into planetary or stellar bodies), the infrared excesses should disappear. Except for chromospheric and photospheric effects, the emergent spectra should then approach those of (slightly) reddened blackbodies. This represents the final stage of pre-main-sequence evolution, in which stars approach the main-sequence on convective-radiative tracks in the H-R diagram.

The evolution of young stellar objects must be a continuous process; thus, it is significant that the observed energy distributions have a continuous span of shapes, from those with negative infrared spectral indices to those with positive ones (LW; Lada 1986; Myers *et al.* 1986). Nevertheless, it is conceptually useful to introduce distinct categories for the major episodes. The results of this work suggest that the spectra of (low-mass) young stellar objects can be understood in terms of the following evolutionary stages:

(a<sub>1</sub>) Protostars during the pure infall phase—steep spectrum infrared sources with negative spectral indices.

(a<sub>2</sub>) Protostars with well-collimated outflows—also sharply declining spectra from the mid-infrared to near-infrared.

(b<sub>1</sub>) T Tauri stars with nebular disks and surrounding dust envelopes of residual infall—double-humped optical and infrared sources if the disks are passive; flat spectra in the mid-infrared and near-infrared with a hump toward lower frequencies if the disks are massive and accreting.

(b<sub>2</sub>) T Tauri stars with nebular disks only—single-humped sources with near-infrared and mid-infrared excesses that have positive to nearly zero spectral indices.

(c) Post-T Tauri stars—reddened blackbodies.

This work was begun during our residence at the Star Formation Program at the Institute for Theoretical Physics. We wish to thank Director Robert Schrieffer for hospitality, support, and computer time at the ITP. We are grateful to Gibor Basri, John Biegging, Martin Cohen, Bruce Elmegreen, Gary Fuller, Susana Lizano, Bob Mathieu, Phil Myers, Barry Rice, Richard Schwartz, Steve Stahler, Peter Strittmatter, Steve Strom, and Rodger Thompson for helpful discussions and suggestions. This work was also funded in part by NSF grant AST83-14682 and in part under the auspices of a special NASA astrophysics theory program which supports a joint Center for Star Formation Studies at NASA/Ames Research Center, U. C. Berkeley, and U. C. Santa Cruz.

## APPENDIX

### HEURISTIC CORRECTION FOR THE EFFECTS OF SCATTERING

With the inclusion of scattering, the equation of transfer reads

$$\mathbf{n} \cdot \nabla I_{\nu}(\mathbf{r}, \mathbf{n}) = \rho \kappa_{\nu}^{\text{abs}} [B_{\nu}(T) - I_{\nu}(\mathbf{r}, \mathbf{n})] + \rho \kappa_{\nu}^{\text{sca}} \left[ \oint \phi_{\nu}(\mathbf{n}', \mathbf{n}) I_{\nu}(\mathbf{r}, \mathbf{n}') d\omega' - I_{\nu}(\mathbf{r}, \mathbf{n}) \right], \quad (\text{A1})$$

where  $\kappa_{\nu}^{\text{abs}}$  and  $\kappa_{\nu}^{\text{sca}}$  are the true absorption and scattering opacities,  $B_{\nu}(T)$  is the Planck function, and  $\phi_{\nu}(\mathbf{n}', \mathbf{n})$  is an angular phase function normalized to unity when integrated over all propagation directions with respect to either  $\mathbf{n}'$  or  $\mathbf{n}$ . At low frequencies, where the scattering is equally backward and forward,

$$\oint \mathbf{n} \phi_{\nu}(\mathbf{n}', \mathbf{n}) d\omega = 0, \quad (\text{A2})$$

we obtain upon taking the zeroth and first angular moments of equation (A1):

$$\nabla \cdot \mathbf{F}_\nu = \rho \kappa_\nu^{\text{abs}} [4\pi B_\nu(T) - c E_\nu], \quad (\text{A3a})$$

$$c \nabla \cdot \mathbf{P}_\nu = -\rho (\kappa_\nu^{\text{abs}} + \kappa_\nu^{\text{sca}}) \mathbf{F}_\nu, \quad (\text{A3b})$$

where we have denoted the monochromatic energy density, flux vector, and pressure tensor by  $E_\nu$ ,  $\mathbf{F}_\nu$ , and  $\mathbf{P}_\nu$ , respectively. The substitution of equation (A3b) into equation (A3a) results in the second-order partial differential equation,

$$\frac{1}{\rho \kappa_\nu} \nabla \cdot \left( \frac{1}{\rho \kappa_\nu} \nabla \cdot \mathbf{P}_\nu \right) = \frac{1}{1 + \kappa_\nu^{\text{sca}}/\kappa_\nu^{\text{abs}}} \left[ E_\nu - \frac{4\pi}{c} B_\nu(T) \right], \quad (\text{A4})$$

where  $\kappa_\nu \equiv \kappa_\nu^{\text{abs}} + \kappa_\nu^{\text{sca}}$  is the extinction coefficient.

We wish heuristically to convert a problem without scattering to one with scattering by using the following trick. Rowan-Robinson's (1980) compilation of scattering and absorbing efficiencies in the optical and near-infrared implies that our adopted mixture of silicate and graphite grains satisfies the approximate formula:  $\kappa_\nu^{\text{sca}}/\kappa_\nu^{\text{abs}} = (v/v_0)^3/[1 + 12(v/v_0)]$  with  $v_0 = 10^{14}$  Hz. Since the extinction is mostly accumulated at  $R_C \gg r_d$ , we can ignore the variation of  $\kappa_\nu^{\text{sca}}/\kappa_\nu^{\text{abs}}$  which arises because silicate grains are destroyed at lower temperatures than graphite. We may then define an effective opacity,

$$\kappa_\nu' \equiv (1 + \kappa_\nu^{\text{sca}}/\kappa_\nu^{\text{abs}})^{-1/2} \kappa_\nu = \left[ 1 + \frac{(v/v_0)^3}{1 + 12(v/v_0)} \right]^{-1/2} \kappa_\nu, \quad (\text{A5})$$

that differs substantially from  $\kappa_\nu$  only for  $v > 10^{14}$  Hz. Equation (A4) now becomes

$$\frac{1}{\rho \kappa_\nu'} \nabla \cdot \left( \frac{1}{\rho \kappa_\nu'} \nabla \cdot \mathbf{P}_\nu \right) = \left[ E_\nu - \frac{4\pi}{c} B_\nu(T) \right]. \quad (\text{A6})$$

The variable closure factors relating  $\mathbf{P}_\nu$  to  $E_\nu$  (and  $\mathbf{F}_\nu$ ) will remain the same if  $\kappa_\nu^{\text{sca}} \ll \kappa_\nu^{\text{abs}}$ . Equation (A6) then shows that a treatment (like that of AS) for the integrated light which attributes all the extinction to pure absorption can be transformed to one which includes (a little bit of) scattering by the simple expedient of replacing  $\kappa_\nu$ , as given by Figure 1 of AS, with  $\kappa_\nu'$ , as given by equation (A5). True scattering removes photons from their original propagation directions, but on average the unabsorbed photons still emerge within the observing beam if the source remains unsolved, as will be marginally true even at optical frequencies for ground-based observations if the protostellar candidate has an effective size  $R_C \approx 10^2$  AU and lies at a distance  $> 10^2$  pc. Mimicking this effect by reducing the effective extinction probably works better numerically than indicated by the above derivation. Interstellar dust grains tend to scatter radiation at optical frequencies (where  $\kappa_\nu^{\text{sca}} \approx \kappa_\nu^{\text{abs}}$ ) strongly in the forward direction (Jones 1973). If  $\phi_\nu(\mathbf{n}', \mathbf{n})$  approached a delta function  $\delta(\mathbf{n}' - \mathbf{n})$ , the scattering source and sink terms in equation (A1) would exactly cancel, and the effective opacity should equal  $\kappa_\nu^{\text{abs}}$ . In practice, the forward peaking cannot be so extreme, and equation (A5), which gives a correction factor of  $(\kappa_\nu^{\text{abs}}/\kappa_\nu)^{1/2}$  instead of  $\kappa_\nu^{\text{abs}}/\kappa_\nu$ , would represent a geometric mean between applying no correction for scattering and the maximum possible.

#### REFERENCES

- Abt, H. A. 1983, *Ann. Rev. Astr. Ap.*, **21**, 343.  
 Adams, F. C., and Shu, F. H. 1986, *Ap. J.*, **308**, 836 (AS).  
 Appenzeller, I., and Tscharnuter, W. 1974, *Astr. Ap.*, **30**, 423.  
 Batrla, W., and Menten, K. M. 1985, *Ap. J. (Letters)*, **298**, L19.  
 Beckwith, S., Sargent, A. I., Scoville, N. Z., Masson, C. R., Zuckerman, B., and Phillips, T. T. 1986, *Ap. J.*, **309**, 755.  
 Beichman, C. A., Myers, P. C., Emerson, J. P., Harris, S., Mathieu, R., Benson, P. J., and Jennings, R. E. 1986, *Ap. J.*, **307**, 337.  
 Biegging, J., Cohen, M., and Schwartz, P. 1984, *Ap. J.*, **282**, 699.  
 Calvet, N., Basri, G., and Kuhl, L. V. 1984, *Ap. J.*, **277**, 725.  
 Cassen, P., and Moosman, A. 1981, *Icarus*, **48**, 353.  
 Cassen, P., Shu, F. H., and Terebey, S. 1985, in *Protostars and Planets II*, ed. D. C. Black and M. S. Matthews (Tucson: University of Arizona Press), p. 448.  
 Chini, R. 1981, *Astr. Ap.*, **99**, 346.  
 Cohen, M. 1986, preprint.  
 Cohen, M., Beiging, J. H., and Schwartz, P. 1982, *Ap. J.*, **253**, 707.  
 Cohen, M., and Kuhl, L. V. 1979, *Ap. J. Suppl.*, **41**, 743.  
 Cohen, M., Harvey, P. M., Schwartz, R. D., and Wilking, B. A. 1984, *Ap. J.*, **278**, 671.  
 Cohen, M., and Schwartz, R. D. 1983, *Ap. J.*, **265**, 877.  
 Cudworth, K. M., and Herbig, G. H. 1979, *A. J.*, **84**, 548.  
 Davidson, J. A., and Jaffe, D. T. 1984, *Ap. J. (Letters)*, **277**, L13.  
 Draine, B. T., and Lee, H. M. 1984, *Ap. J.*, **285**, 89.  
 Dyck, H. M., Simon, T., and Zuckerman, B. 1982, *Ap. J. (Letters)*, **255**, L103.  
 Elias, J. A. 1978a, *Ap. J.*, **224**, 453.  
 ———. 1978b, *Ap. J.*, **224**, 857.  
 Friedjung, M. 1985, *Astr. Ap.*, **146**, 366.  
 Hanson, R. B., Jones, B. F., and Lin, D. N. C. 1983, *Ap. J. (Letters)*, **270**, L27.  
 Hartmann, L., and Kenyon, S. J. 1985, *Ap. J.*, **299**, 462.  
 Hartmann, L., Hewett, R., Stahler, S., and Mathieu, R. 1986, *Ap. J.*, **309**, 275.  
 Hayashi, C., Hoshi, R., and Sugimoto, D. 1962, *Prog. Theoret. Phys. Suppl.*, No. 22.  
 Herbig, G. H. 1977, *Ap. J.*, **217**, 693.  
 Jones, T. W. 1973, *Pub. A.S.P.*, **85**, 811.  
 Kahn, F. 1974, *Astr. Ap.*, **37**, 149.  
 Kaifu, N., et al. 1984, *Astr. Ap.*, **134**, 7.  
 Lada, C. J. 1986, in *IAU Symposium 115, Star Forming Regions*, ed. M. Peimbert and J. Jugaku (Dordrecht: Reidel), in press.  
 Lada, C. J., and Wilking, B. A. 1980, *Ap. J.*, **238**, 620.  
 ———. 1984, *Ap. J.*, **287**, 610 (LW).  
 Larson, R. B. 1969, *M.N.R.A.S.*, **145**, 271.  
 Larson, R. B., and Starrfield, S. 1971, *Astr. Ap.*, **13**, 190.  
 Lin, D. N. C., and Papaloizou, J. 1985, in *Protostars and Planets II*, ed. D. C. Black and M. S. Matthews (Tucson: University of Arizona Press), p. 981.  
 Lizano, S., and Shu, F. H. 1986, in preparation.  
 Loren, R. B., Sandqvist, A., and Wootten, A. 1983, *Ap. J.*, **270**, 620.  
 Lynden-Bell, D., and Pringle, J. E. 1974, *M.N.R.A.S.*, **168**, 603.  
 Mendoza, E. E. V. 1966, *Ap. J.*, **143**, 1010.  
 ———. 1968, *Ap. J.*, **151**, 977.  
 Menten, K. M., and Walmsley, C. M. 1985, *Astr. Ap.*, **146**, 369.  
 Mercer-Smith, J. A., Cameron, A. G. W., and Epstein, R. I. 1984, *Ap. J.*, **287**, 445.  
 Mouchovias, T. Ch., and Paleologou, E. V. 1979, *Ap. J.*, **230**, 204.  
 Mundt, R., and Fried, J. W. 1983, *Ap. J. (Letters)*, **274**, L83.  
 Mundt, R., Stocke, J., Strom, S. E., and Anderson, E. R. 1985, *Ap. J. (Letters)*, **297**, L41.  
 Myers, P. C. 1986, in *IAU Symposium 115, Star Forming Regions*, ed. M. Peimbert and J. Jugaku (Dordrecht: Reidel), in press.  
 Myers, P. C., and Benson, P. J. 1983, *Ap. J.*, **266**, 309.  
 Myers, P. C., Fuller, G. A., Mathieu, R. D., Beichman, C. A., Benson, P. J., and Schild, R. D. 1986, in preparation.  
 Rowan-Robinson, M. 1980, *Ap. J. Suppl.*, **44**, 403.  
 Rucinski, S. M. 1985, *A. J.*, **90**, 2321.  
 Rydgren, A. E., Schmelz, J. T., Zak, D. S., and Vrba, F. J. 1984, *Broad Band Spectral Energy Distributions of T Tauri Stars in the Taurus-Auriga Region*, *Pub. US Naval Obs.*, Vol. **25**, Part 1.  
 Rydgren, A. E., Strom, S. E., and Strom, K. M. 1976, *Ap. J. Suppl.*, **30**, 307.

- Sandqvist, Aa., and Bernes, C. 1980, *Astr. Ap.*, **89**, 187.  
 Sargent, A. I., and Beckwith, S. 1986, in preparation.  
 Schwartz, P. R., Simon, T. B., Zuckerman, B., and Howell, R. R. 1984, *Ap. J. (Letters)*, **280**, L23.  
 Shu, F. H. 1977, *Ap. J.*, **214**, 488.  
 ———. 1985, in *IAU Symposium 106, The Milky Way*, ed. H. van Woerden, W. B. Burton, and R. J. Allen (Dordrecht: Reidel), p. 561.  
 Shu, F. H., Lizano, S., and Adams, F. C. 1986, in *IAU Symposium 115, Star Forming Regions*, ed. M. Peimbert and J. Jugaku (Dordrecht: Reidel), in press.  
 Shu, F. H., and Terebey, S. 1984, in *Cool Stars, Stellar Systems, and the Sun*, ed. S. Baliunas and L. Hartmann (Berlin: Springer-Verlag), p. 78.  
 Smith, H. A., Thronson, H. A., Lada, C. J., Harper, D. A., Lowenstein, R. F., and Smith, J. 1982, *Ap. J.*, **258**, 170.  
 Snell, R. L. 1981, *Ap. J. Suppl.*, **45**, 121.  
 Snell, R. L., Bally, J., Strom, S. E., and Strom, K. M. 1985, *Ap. J.*, **290**, 587.  
 Snell, R. L., Loren, R. B., and Plambeck, R. L. 1980, *Ap. J. (Letters)*, **239**, L17.  
 Stahler, S. 1983, *Ap. J.*, **274**, 822.  
 Stahler, S. 1984, in *Cool Stars, Stellar Systems, and the Sun*, ed. S. Baliunas and L. Hartmann (Berlin: Springer-Verlag), p. 90.  
 Stahler, S. W., Shu, F. H., and Taam, R. E. 1980, *Ap. J.*, **241**, 637.  
 Strom, S. E., Grasdalen, G. L. and Strom, K. M. 1974, *Ap. J.*, **191**, 111.  
 Strom, S. E., Strom, K. M., and Vrba, F. J. 1976, *A.J.*, **83**, 320.  
 Terebey, S., Shu, F. H., and Cassen, P. 1984, *Ap. J.*, **286**, 529.  
 Torrelles, J. M., Rodriguez, L. F., Cantó, J., Carral, P., Marcaide, J., Moran, J. M., and Ho, P. T. P. 1983, *Ap. J.*, **274**, 214.  
 Vogel, S., and Kuhl, L. V. 1981, *Ap. J.*, **245**, 960.  
 Vrba, J. F., Strom, K. M., Strom, S. E., and Grasdalen, G. L. 1975, *Ap. J.*, **197**, 77.  
 Wilking, B. A., and Lada, C. J. 1983, *Ap. J.*, **274**, 698.  
 Winkler, K-H., and Newman, M. J. 1980a, *Ap. J.*, **236**, 201.  
 ———. 1980b, *Ap. J.*, **238**, 311.  
 Wolfire, M. G., and Cassinelli, J. P. 1986, *Ap. J.*, **310**, 207.  
 Yorke, H. W., and Krugel, E. 1977, *Astr. Ap.*, **54**, 183.  
 Young, E. T., Lada, C. J., and Wilking, B. A. 1986, *Ap. J. (Letters)*, **304**, L45.

FRED C. ADAMS: Physics and Astronomy Departments, University of California, Berkeley, CA 94720

CHARLES J. LADA: Steward Observatory, University of Arizona, Tucson, AZ 85721

FRANK H. SHU: Astronomy Department, University of California, Berkeley, CA 94720